The University of Manitoba

A PROTON MAGNETIC RESONANCE STUDY OF THE HINDERED ROTATION IN α,α,α',α',3,4,6-HEPTACHLORO-ORTHO-XYLENE

by

Walter Edward Hiebert

A Thesis

Submitted to

the Faculty of Graduate Studies and Research

The University of Manitoba

In Partial Fulfillment

of the Requirements of the Degree

MASTER OF SCIENCE

Winnipeg, Manitoba

July, 1976

"A PROTON MAGNETIC RESONANCE STUDY

OF THE HINDERED ROTATION IN

α,α,α',α', 3,4,6-HEPTACHLORO-ORTHO-XYLENE"

by

WALTER EDWARD HIEBERT

A dissertation submitted to the Faculty of Graduate Studies of the University of Manitoba in partial fulfillment of the requirements of the degree of

MASTER OF SCIENCE

TO MY WIFE MARLENE

ACKNOWLEDGMENTS

I express my deep gratitude to Dr. Harold Hutton for patient guidance during the time of this study.

I am also grateful to Dr. Ted Schaefer for his valuable counsel and the use of his N.M.R. facilities. The discussions with Dr. Brian Rowbotham, Dr. James Peeling, Mr. Werner Danchura and Mr. Kalvin Chum have been very beneficial.

Special thanks go to Dr. Victor Marks of Central Research Department, Hooker Chemical Corporation for supplying the compound used in the study.

Finally, the moral support of Prof. Lawrence Swyers and of Dr. Fred Barth at the University of Winnipeg are gratefully acknowledged.

ABSTRACT

A high resolution proton magnetic resonance investigation of the hindered rotation of the dichloromethyl groups as a function of temperature in α,α,α',α',3,4,6-heptachloro-ortho-xylene (HCOX) has been conducted using dynamic nuclear magnetic resonance (DNMR) line shape analysis, supplemented with a homonuclear double resonance saturation transfer technique. The rate process in HCOX involves a coupled rotation of two substituted methyl groups and the nonmutual exchange of the three pairs of protons between two approximately equally populated conformations. The activation parameters are calculated using the Arrhenius and transition state theories from the rate constants of the hindered rotation, obtained over a temperature range of 268°K to 369°K. The values obtained for a five mole per cent solution of HCOX in methylcyclohexane are: activation energy, Ea, equals 15.3 ± 0.3 kcal $mole^{-1}$, enthalpy of activation, $\Delta H^{\neq}$, equals 14.6 ± 0.3 kcal $mole^{-1}$, activation entropy, $\Delta S^{\neq}$, equals -8.8 ± 0.8 e.u., and the free energy of activation at 298°K, $\Delta G^{\neq}$, equals 17.2 ± 0.3 kcal $mole^{-1}$. The results are compared with previously reported values for HCOX and with other compounds having similar barriers to hindered rotation.

TABLE OF CONTENTS

LIST OF TABLES

LIST OF FIGURES

I. INTRODUCTION

The use of nuclear magnetic resonance (N.M.R.) in the determination of structures of molecules and in conformational studies has increased greatly in recent years (1) as both continuous-wave and pulsed N.M.R. spectrometers are becoming more generally available.

This thesis will consider only the application of continuous-wave N.M.R. spectroscopy to the rate process governing the conformational changes in a molecule. The term conformation or conformer refers to any relative spatial arrangement of atoms, or groups of atoms, occurring with a rotation about a bond (2), whereas configuration refers to the relative spatial arrangement of the atoms bonded to each other (3); bonds must be broken and re-formed to interchange configurations. At room temperature, configurations are normally stable and assignment of a lifetime is meaningless; for conformers, there is a large range of lifetimes which reflect the different rotational energies required. Hence, some conformers with long lifetimes, such as the ortho-substituted biphenyls, may be resolved at room temperature (4) while others, such as ethane, remain inseparable even at very low temperatures.

N.M.R. line shapes are sensitive to lifetimes from 10 μsec to 10 seconds (5), or rate processes occurring with a frequency of $0.1 - 10^5$ sec^{-1}. To a first approximation the line shape changes occurring below $+100^{o}C$ can be attributed to conformational changes with short lifetimes at room temperature, while those occurring over $+150^{o}C$ will normally have such long lifetimes at room temperature that separation of the conformers should be possible (4).

The experimental spectra obtained as a function of temperature

can be compared with computer-generated spectra to obtain the exchange rate constant, k (6,7). Under conditions of fast exchange, $k >> \Delta\nu$, where $\Delta\nu$ is the frequency separating the peak positions of the conformers, the spectrum shows peaks at the average position for the two conformers; at the slow exchange limit, $k << \Delta\nu$, the spectra displays a distinct set of peaks for each conformer. In the intermediate region the spectra are sensitive to temperature changes; as k increases from the lower to the upper limit the peaks for each proton broaden, then coalesce, and finally yield a single line with a gradually decreasing line width. At lower temperatures the exchange rate and the change in the appearance of a spectrum with and without exchange becomes increasingly difficult to detect. A similar observation can be made for the temperature region approaching the upper limit for k. The large errors in using the visual matching technique in the slow exchange region are substantially reduced by employing the decay and recovery curves of the saturation transfer technique (8,9) to obtain the exchange rate constants; thus effectively extending the lower limit of the temperature range amenable to study using N.M.R. spectroscopy.

This thesis deals specifically with the application of dynamic nuclear magnetic resonance (DNMR) to the investigation of the rate process involved in the hindered rotation of $\alpha,\alpha,\alpha',\alpha'$,3,4,6-heptachloro-ortho-xylene (HCOX). The absorption peaks were assigned to two conformers under conditions of slow exchange. Under conditions of intermediate exchange the rate constants were obtained by fitting the experimental spectra to the computer-generated spectra generated by the

program DNMR2 (10,11). At slower exchange rates the k values were determined from the lifetimes τ and the spin-lattice relaxation times T_1 using the method described by Anet and Bourn (9). The activation parameters and thermodynamic values were calculated using both the Arrhenius and the absolute reaction rate theories (12).

II. THEORETICAL DISCUSSION

A. Introduction

Early approaches to the theoretical description of N.M.R. spectra were those of Bloch (13-17) and of Hamilton (18). The Bloch equations are useful for calculating line shapes for uncoupled spin systems (19). The spin Hamiltonian is used to determine the positions and the intensities of the spectral lines from chemical shifts and coupling constants; however, it may not be used to calculate line shapes when an exchange process is involved.

Another treatment which incorporates elements of these two earlier ones was suggested by Kaplan (20) and developed by Alexander (21). This method is based on the equation of motion of a so-called nuclear spin density matrix for a dynamic system which need not be completely specified. It is less complex than the Bloch equations for simple systems and can also be used to obtain useful information from complicated systems by making successively more drastic assumptions in the calculation. This density matrix method, including the effects of spin-spin coupling between nuclei is briefly discussed in section B following the procedure of Whitesides (22).

Section C contains the theory necessary to extract rate constants from the double resonance saturation transfer technique and this chapter concludes with a discussion of activation parameter calculations.

B. The Density Matrix Treatment

Consider a system at some instant in time described by a wave function, Ψ, where Ψ is expanded into a complete set of orthonormal time-independent basis functions, ϕ_i

$$\Psi = \sum_i c_i \phi_i \qquad 2.1$$

If Ψ varies as a function of time the coefficients, c_i, of the orthonormal functions must be time-dependent. The expectation value of an operator such as the magnetization in the x-direction, M_x, can be written as

$$\langle M_x \rangle = \sum_{m,n} c_m^* c_n \, (\phi_m \, |M_x| \, \phi_n) \qquad 2.2$$

where c_m^* is the complex conjugate of c_m. Since the basis functions are the same for all Ψ, the last term, $(\phi_m \, |M_x| \, \phi_n)$, will remain constant for any operator. Thus $\langle M_x \rangle$ will depend on the product of the coefficients which correspond to the observable properties of a system. The $c_m^* c_n$ terms can be placed in matrix form to calculate the expectation value of an operator. The expectation value for an ensemble of molecules, $\langle \overline{M_x} \rangle$, will be given by $\overline{c_m^* c_n}$. Thus an expectation value can be obtained without having the maximum information available from the state of the system. The matrix formed by the quantities, $c_m^* c_n$, is defined as a density matrix of an operator, ρ, given by

$$(\phi_n \, |\rho| \, \phi_m) = \overline{c_n c_m^*} \qquad 2.3$$

or, in matrix form for a two-spin system,

$$\rho = \begin{bmatrix} \rho_{11} & \rho_{12} & \rho_{13} & \rho_{14} \\ \rho_{21} & \rho_{22} & \rho_{23} & \rho_{24} \\ \rho_{31} & \rho_{32} & \rho_{33} & \rho_{34} \\ \rho_{41} & \rho_{42} & \rho_{43} & \rho_{44} \end{bmatrix} \qquad 2.4$$

Since ρ is an Hermitian operator the expectation value for the magnetization in the x-direction will be determined by the diagonal elements

$$\langle M_x \rangle = \mathrm{Tr}\ \rho\ M_x = \mathrm{Tr}\ M_x\ \rho \qquad 2.5$$

The time dependent Hamiltonian, H, of the system is

$$\frac{d\Psi}{dt} = -\frac{i}{\hbar} H\ \Psi \qquad 2.6$$

where the time dependent part of the state function Ψ is found in the $\overline{c_n c_m^*}$ terms of the operator ρ. Therefore it is possible to substitute for Ψ and obtain

$$\frac{d\rho}{dt} = \frac{i}{\hbar}\left[\rho,\ H\right] \qquad 2.7$$

One common situation is that of a Hamiltonian consisting of a large time-independent interaction, H_o, and a small time dependent term, H_t. The equation of motion of the matrix then becomes

$$\frac{d\rho}{dt} = \frac{i}{\hbar}\left[\rho,\ H_o + H_t\right] \qquad 2.8$$

in the absence of effects such as exchange and relaxation. These effects can be explicitly included in the expression by writing

$$\frac{d\rho}{dt} = \frac{i}{\hbar}\left[\rho,\ H_o + H_t\right] + \left(\frac{\partial\rho}{\partial t}\right)_{exchange} + \left(\frac{\partial\rho}{\partial t}\right)_{relaxation} \qquad 2.9$$

The following sections deal with each of these terms separately using a two-spin system as an example.

1. The $\frac{i}{\hbar}\left[\rho,\ H_o + H_t\right]$ term

a) Commutator of ρ with H_o

Consider a two-spin system with basis functions $\alpha\alpha$, $\alpha\beta$, $\beta\alpha$, $\beta\beta$, as eigenfunctions of the spin operator, I_z. Since I_z is Hermitian, only diagonal terms need be considered, with

$$\begin{aligned} H_{o11} &= \frac{\gamma H_o(2 - \sigma_1 - \sigma_2)}{2} - \omega + \tfrac{1}{4}J \\ H_{o22} &= -\frac{\gamma H_o}{2}(\sigma_1 - \sigma_2) - \tfrac{1}{4}J \\ H_{o33} &= \frac{\gamma H_o}{2}(\sigma_1 - \sigma_2) - \tfrac{1}{4}J \\ H_{o44} &= -\frac{\gamma H_o(2 - \sigma_1 - \sigma_2)}{2} + \omega + \tfrac{1}{4}J \end{aligned} \qquad 2.10$$

in a rotating framework* with frequency, ω, relative to a fixed position, where γ is the magnetogyric ratio, H_o the static magnetic field, σ the shielding constant, and J the spin-spin coupling constant between the

---

* See appendix for transformation of spin operators to a rotating framework.

two spins.

If the chemical shift between the two spins, δ, is defined by

$$\delta = \frac{\gamma H_0(\sigma_1 - \sigma_2)}{2} \qquad 2.11$$

and the chemical shift midway between the resonant frequencies, Δ, by

$$\Delta = \omega - \frac{\gamma H_0(2 - \sigma_1 - \sigma_2)}{2} \qquad 2.12$$

then the matrix representation is

$$H_0 = \begin{bmatrix} -\Delta+\frac{1}{4}J & 0 & 0 & 0 \\ 0 & \frac{1}{2}\delta-\frac{1}{4}J & \frac{1}{2}J & 0 \\ 0 & \frac{1}{2}J & -\frac{1}{2}\delta-\frac{1}{4}J & 0 \\ 0 & 0 & 0 & \Delta+\frac{1}{4}J \end{bmatrix} \qquad 2.13$$

and the commutator is

$$[\rho, H_0] = \begin{bmatrix} 0 & \rho_{12}(\Delta+\frac{1}{2}\delta-\frac{1}{2}J)+\rho_{13}(\frac{1}{2}J) & \rho_{12}(\frac{1}{2}J)+\rho_{13}(\Delta-\frac{1}{2}\delta-\frac{1}{2}J) & \rho_{14}(2\Delta) \\ \rho_{21}(-\Delta-\frac{1}{2}\delta+\frac{1}{2}J)-\rho_{31}(\frac{1}{2}J) & 0 & \rho_{23}(-\delta)+\rho_{22}(\frac{1}{2}J)-\rho_{33}(\frac{1}{2}J) & \rho_{24}(\Delta-\frac{1}{2}\delta+\frac{1}{2}J)-\rho_{34}(\frac{1}{2}J) \\ \rho_{31}(-\Delta+\frac{1}{2}\delta+\frac{1}{2}J)-\rho_{21}(\frac{1}{2}J) & \rho_{32}(\delta)+\rho_{33}(\frac{1}{2}J)-\rho_{22}(\frac{1}{2}J) & 0 & -\rho_{24}(\frac{1}{2}J)+\rho_{34}(\Delta+\frac{1}{2}\delta+\frac{1}{2}J) \\ \rho_{41}(-2\Delta) & \rho_{42}(-\Delta+\frac{1}{2}\delta-\frac{1}{2}J)+\rho_{43}(\frac{1}{2}J) & \rho_{42}(\frac{1}{2}J)+\rho_{43}(-\Delta-\frac{1}{2}\delta-\frac{1}{2}J) & 0 \end{bmatrix} \qquad 2.14$$

Note that the trace is zero as the constant interaction of H_0 results in a steady state as intuitively suspected.

b) Commutator of ρ with $H_1(t)$

Consider the time-dependent interaction to be expressed as

$$H_1(t) = \sum_j \gamma H_1 \left(I_x(j) \cos \omega t + I_y(j) \sin \omega t \right) \qquad 2.15$$

the interaction between the nuclear magnetic moments and a magnetic field with amplitude H_1 rotating in the x-y plane at a frequency, ω, relative to a fixed laboratory position.

A transformation to the rotating framework* used in the previous section yields

$$H_1(t) = \sum_i \gamma H_1 I_x(i) \qquad 2.16$$

with the matrix representation

$$H_1(t) = \frac{\gamma H_1}{2} \begin{bmatrix} 0 & 1 & 1 & 0 \\ 1 & 0 & 0 & 1 \\ 1 & 0 & 0 & 1 \\ 0 & 1 & 1 & 0 \end{bmatrix} \qquad 2.17$$

As previously indicated, $H_1 << H_0$, and therefore it is possible to obtain an approximate but explicit operator for ρ, to evaluate $[\rho\ H_1(t) - H_1(t)\ \rho]$. It is known that the diagonal terms of ρ are much greater than the off-diagonal terms at all times and that at equilibrium, the off-diagonal elements vanish. In addition, all terms will be multiplied by $\frac{\gamma H_1}{2}$ which will reduce the significance of the off-diagonal

---

* See appendix for transformation of operators to a rotating framework.

elements. Hence only the diagonal terms need be considered for evaluating $[\rho, H_1(t)]$. These correspond to the equilibrium populations of the various states and are given by the Boltzmann factors of the corresponding energy levels. The expression for ρ then is

$$\rho = \frac{\exp\ (-H/kT)}{\sum_n \exp\ (-E_{(n)}/kT)} \qquad 2.18$$

where $H \simeq H_o$. Since $H_o >> H_1$, and assuming the shielding constants contribute a negligible effect, then

$$H \simeq \gamma\hbar H_o(I_{z1} + I_{z2}) \qquad 2.19$$

Substituting 2.19 into the expression for ρ and expanding to first order yields

$$\rho = \frac{1}{N}\left(1 - \frac{\gamma\hbar H_o F_z}{kT}\right) \qquad 2.20$$

where $F_z = I_{z1} + I_{z2}$ and $N = \sum_n \exp\ (-E_{(n)}/kT)$. Using this expression the matrix representation is

$$\rho = \frac{1}{N}\begin{bmatrix} 1 - \frac{\hbar\gamma H_o}{kT} & 0 & 0 & 0 \\ 0 & 1 & 0 & 0 \\ 0 & 0 & 1 & 0 \\ 0 & 0 & 0 & 1 + \frac{\gamma\hbar H_o}{kT} \end{bmatrix} \qquad 2.21$$

and the commutator can then be calculated as

$$\left[\rho\, H_1(t) - H_1(t)\, \rho\right] = \frac{\gamma^2 \hbar H_0 H_1}{2NkT} \begin{bmatrix} 0 & -1 & -1 & 0 \\ +1 & 0 & 0 & -1 \\ +1 & 0 & 0 & -1 \\ 0 & +1 & +1 & 0 \end{bmatrix} \qquad 2.22$$

2. The $\left(\frac{\partial \rho}{\partial t}\right)_{\text{exchange}}$ term

When two of the spins exchange sites the effect is the same as if they exchanged indices, or labelled positions, of the spin. Such an effect is assigned to a permutation operator, P. The effect of P on the basis functions for a system exchanging between two sites can be represented by a matrix

$$P = \begin{bmatrix} 1 & 0 & 0 & 0 \\ 0 & 0 & 1 & 0 \\ 0 & 1 & 0 & 0 \\ 0 & 0 & 0 & 1 \end{bmatrix} \qquad 2.23$$

A second exchange of sites would restore the system to its initial state. Thus $P \cdot P = I$, which implies that $P = P^{-1}$. Therefore, after the exchange one could write a matrix, $\rho' = P^{-1}\rho P$. If the lifetime of the proton at each site is given by τ, the rate change of ρ due to exchange is

$$\left(\frac{\partial \rho}{\partial t}\right)_{\text{exchange}} = \frac{\rho_{\text{after}} - \rho_{\text{before}}}{\tau} = \frac{\rho' - \rho}{\tau} \qquad 2.24$$

for a constant rate of exchange at constant temperature. Evaluation of 2.24 requires that ρ' be obtained in matrix form

$$\rho' = P\rho P = \begin{bmatrix} \rho_{11} & \rho_{13} & \rho_{12} & \rho_{14} \\ \rho_{31} & \rho_{33} & \rho_{32} & \rho_{34} \\ \rho_{21} & \rho_{23} & \rho_{22} & \rho_{24} \\ \rho_{41} & \rho_{43} & \rho_{42} & \rho_{44} \end{bmatrix} \qquad 2.25$$

Then

$$\left(\frac{\partial\rho}{\partial t}\right)_{\text{exchange}} = \frac{\rho' - \rho}{\tau} = \frac{1}{\tau}\begin{bmatrix} 0 & \rho_{13}-\rho_{12} & \rho_{12}-\rho_{13} & 0 \\ \rho_{31}-\rho_{21} & \rho_{33}-\rho_{22} & \rho_{32}-\rho_{23} & \rho_{34}-\rho_{24} \\ \rho_{21}-\rho_{31} & \rho_{23}-\rho_{33} & \rho_{22}-\rho_{33} & \rho_{24}-\rho_{34} \\ 0 & \rho_{43}-\rho_{42} & \rho_{42}-\rho_{43} & 0 \end{bmatrix}$$

2.26

3. The $\left(\frac{\partial\rho}{\partial t}\right)_{\text{relaxation}}$ term

The process of maintaining or restoring thermal equilibrium in the spin system through an exchange of energy between the nuclei under investigation and the surrounding molecules is the spin-lattice relaxation. Thermal motion produces randomly fluctuating magnetic fields which can interact with the magnetic moments of the molecules with which it experiences thermal contact. If any component of this fluctuating field is at the Larmor frequency, then transitions among the energy levels are possible and the Boltzmann distribution is restored. After a perturbation that disturbed the populations of the energy levels, the restoration to equilibrium conditions are characterized by a time constant, T_1, defined as the spin-lattice relaxation time.

In the problem under consideration, the spin-lattice relaxation time affects the diagonal terms of ρ by the expression

$$\left(\frac{\rho_0 - \rho}{T_1}\right)_{\text{diagonal}} \qquad 2.27$$

where ρ_0 is the equilibrium value of ρ.

Relaxation is also affected by the presence of local internal fields originating from neighbouring magnetic moments in the sample. Unless these moments move about rapidly, the small, local contributions will change the effective field strength of the precessing nuclei, and these different field strengths produce different precessional frequencies. Thus they quickly lose phase and thermal equilibrium is established. Since the energy changes are confined entirely to the spin system, this is called spin-spin relaxation, characterized by a time constant, T_2. In the problem under consideration the spin-spin relaxation time affects only the off-diagonal terms of ρ by the expression

$$\left(\frac{-\rho}{T_2}\right)_{\text{off-diagonal}} \qquad 2.28$$

which decays to zero as thermal equilibrium is restored. There are no common terms between the spin-lattice and spin-spin relaxation times and they can be combined in matrix form to obtain

$$\left(\frac{\partial\rho}{\partial t}\right)_{\text{relaxation}} = \begin{bmatrix} \frac{1}{T_1}(\rho_o-\rho)_{11} & -\rho_{12}/T_2 & -\rho_{13}/T_2 & -\rho_{14}/T_2 \\ -\rho_{21}/T_2 & \frac{1}{T_1}(\rho_o-\rho)_{22} & -\rho_{23}/T_2 & -\rho_{24}/T_2 \\ -\rho_{31}/T_2 & -\rho_{32}/T_2 & \frac{1}{T_1}(\rho_o-\rho)_{33} & -\rho_{34}/T_2 \\ -\rho_{41}/T_2 & -\rho_{42}/T_2 & -\rho_{43}/T_2 & \frac{1}{T_1}(\rho_o-\rho)_{44} \end{bmatrix} \qquad 2.29$$

4. Calculation of line shape

a) Introduction

In the N.M.R. experiment the sample is irradiated with a radiofrequency (rf) field, $H_1(t)$, rotating in the x-y plane with the constant magnetic field, H_o, in the z-direction. The magnetization induced in the sample is measured by receiver coils perpendicular to both the transmitter coils and to the static field. The absorption of energy due to the net upward transitions corresponds to a raising operator given by

$$I^+ \equiv I_x + iI_y \qquad 2.30$$

and since the mean value of an observable is given by the diagonal terms, it is the trace of this operator with the density matrix that is important

$$\mathrm{Tr}(\rho I^+) = \mathrm{Tr}(I^+\rho) \qquad 2.31$$

b) Matrix representation for I^+

Using the same orthonormal functions as before and the conventional function of the operator, the matrix representation is

$$I^+ = \begin{bmatrix} 0 & 1 & 1 & 0 \\ 0 & 0 & 0 & 1 \\ 0 & 0 & 0 & 1 \\ 0 & 0 & 0 & 0 \end{bmatrix} \qquad 2.32$$

with the product $I^+\rho$ given by

$$I^+\rho = \begin{bmatrix} 0 & 1 & 1 & 0 \\ 0 & 0 & 0 & 1 \\ 0 & 0 & 0 & 1 \\ 0 & 0 & 0 & 0 \end{bmatrix} \begin{bmatrix} \rho_{11} & \rho_{12} & \rho_{13} & \rho_{14} \\ \rho_{21} & \rho_{22} & \rho_{23} & \rho_{24} \\ \rho_{31} & \rho_{32} & \rho_{33} & \rho_{34} \\ \rho_{41} & \rho_{42} & \rho_{43} & \rho_{44} \end{bmatrix}$$

$$= \begin{bmatrix} \rho_{21}+\rho_{31} & \rho_{22}+\rho_{32} & \rho_{23}+\rho_{33} & \rho_{24}+\rho_{34} \\ \rho_{41} & \rho_{42} & \rho_{43} & \rho_{44} \\ \rho_{41} & \rho_{42} & \rho_{43} & \rho_{44} \\ 0 & 0 & 0 & 0 \end{bmatrix} \qquad 2.33$$

and

$$Tr(I^+\rho) = \rho_{21} + \rho_{31} + \rho_{42} + \rho_{43} = \langle I^+ \rangle \qquad 2.34$$

To determine $\frac{d\rho}{dt}$ only the four terms $\frac{d\rho_{21}}{dt}$, $\frac{d\rho_{31}}{dt}$, $\frac{d\rho_{42}}{dt}$ and $\frac{d\rho_{43}}{dt}$ need to to be evaluated.

c) Calculation of spectral points

If it is assumed that the spectrum is swept slowly enough so as to cause a negligible change in the signal amplitude with time, then

$$\frac{d\rho}{dt} \simeq 0; \text{ that is, } \frac{d\rho_{21}}{dt} = \frac{d\rho_{31}}{dt} = \frac{d\rho_{42}}{dt} = \frac{d\rho_{43}}{dt} \simeq 0 \qquad 2.35$$

Evaluating each of these from the previously-determined matrices for ρ one obtains the four equations

$$\frac{d\rho_{21}}{dt} = \frac{\rho_{31}-\rho_{21}}{\tau} - \frac{\rho_{21}}{T_2} + i(-\Delta-\tfrac{1}{2}\delta+\tfrac{1}{2}J)\rho_{21} - i(\tfrac{1}{2}J)\rho_{31} + iC = 0$$

$$\frac{d\rho_{31}}{dt} = \frac{\rho_{21}-\rho_{31}}{\tau} - \frac{\rho_{31}}{T_2} + i(-\Delta+\tfrac{1}{2}\delta+\tfrac{1}{2}J)\rho_{31} - i(\tfrac{1}{2}J)\rho_{21} + iC = 0$$

$$\frac{d\rho_{42}}{dt} = \frac{\rho_{43}-\rho_{42}}{\tau} - \frac{\rho_{42}}{T_2} + i(-\Delta+\tfrac{1}{2}\delta-\tfrac{1}{2}J)\rho_{42} + i(\tfrac{1}{2}J)\rho_{43} + iC = 0$$

$$\frac{d\rho_{43}}{dt} = \frac{\rho_{42}-\rho_{43}}{\tau} - \frac{\rho_{43}}{T_2} + i(-\Delta-\tfrac{1}{2}\delta-\tfrac{1}{2}J)\rho_{43} + i(\tfrac{1}{2}J)\rho_{42} + iC = 0 \qquad 2.36$$

where $C = \dfrac{\gamma^2\hbar H_0 H_1}{2NkT}$

There are no cross terms between the pairs (ρ_{21}, ρ_{31}) and (ρ_{42}, ρ_{43}) and one obtains

$$\rho_{21} = \frac{C\left(-\Delta+\tfrac{1}{2}\delta+J+\frac{2i}{\tau}+\frac{i}{T_2}\right)}{-\Delta^2+\tfrac{1}{4}\delta^2+\Delta J+\frac{i}{\tau}(2\Delta)+\frac{i}{T_2}\left(2\Delta-J-\frac{2i}{\tau}-\frac{i}{T_2}\right)}$$

$$\rho_{31} = \frac{C\left(-\Delta-\tfrac{1}{2}\delta+J+\frac{2i}{\tau}+\frac{i}{T_2}\right)}{-\Delta^2+\tfrac{1}{4}\delta^2+\Delta J+\frac{i}{\tau}(2\Delta)+\frac{i}{T_2}\left(2\Delta-J-\frac{2i}{\tau}-\frac{i}{T_2}\right)}$$

2.37

$$\rho_{42} = \frac{C\left(-\Delta-\tfrac{1}{2}\delta-J+\frac{2i}{\tau}+\frac{i}{T_2}\right)}{-\Delta^2+\tfrac{1}{4}\delta^2-\Delta J+\frac{i}{\tau}(2\Delta)+\frac{i}{T_2}\left(2\Delta+J-\frac{2i}{\tau}-\frac{i}{T_2}\right)}$$

$$\rho_{43} = \frac{C\left(-\Delta+\tfrac{1}{2}\delta-J+\frac{2i}{\tau}+\frac{i}{T_2}\right)}{-\Delta^2+\tfrac{1}{4}\delta^2-\Delta J+\frac{i}{\tau}(2\Delta)+\frac{i}{T_2}\left(2\Delta+J-\frac{2i}{\tau}-\frac{i}{T_2}\right)}$$

Adding terms with common denominators yields

$$\rho_{21}+\rho_{31} = \frac{2C\left(-\Delta+J+\frac{2i}{\tau}+\frac{i}{T_2}\right)}{-\Delta^2+\tfrac{1}{4}\delta^2+\Delta J+\frac{i}{\tau}(2\Delta)+\frac{i}{T_2}\left(2\Delta-J-\frac{2i}{\tau}-\frac{i}{T_2}\right)}$$

2.38

and

$$\rho_{42}+\rho_{43} = \frac{2C\left(-\Delta-J+\frac{2i}{\tau}+\frac{i}{T_2}\right)}{-\Delta^2+\tfrac{1}{4}\delta^2+\Delta J+\frac{i}{\tau}(2\Delta)+\frac{i}{T_2}\left(2\Delta+J-\frac{2i}{\tau}-\frac{i}{T_2}\right)}$$

2.39

where the sum $\rho_{21} + \rho_{31} + \rho_{42} + \rho_{43}$ is the expression for the magnitude

of the induced magnetization in the x-y plane. The real part of each expression corresponds to a dispersion signal and the imaginary part corresponds to the absorption signal commonly recorded. Adding the imaginary parts of equations 2.38 and 2.39, the expression for the line shape of the absorption signal in the x-y plane is obtained. The resulting calculation, although tedious by hand, can readily be performed by a computer (5) and the resultant data plotted to obtain a spectrum to be matched with an experimental one. The purpose is to find activation rate parameters (τ or k) by matching theoretical spectra to experimental ones and using these to calculate the thermodynamic properties of the system under study (12).

C. Double Resonance Saturation Transfer Method

1. Introduction

The determination of accurate rate constants by matching experimental and computer-simulated spectra when the rate process is slow is difficult. An alternative procedure for the slow exchange region, the method of saturation transfer, was proposed by Forsen and Hoffman (8,23,24) and developed by Anet and Bourn (9). This section presents a brief theory of the method for the slow exchange of a single spin between site A and site B (following the method outlined in reference 9).

It is possible to change the relative populations of the two spin states of a proton by irradiation with a strong rf field at its resonance frequency. If the protons at site A are saturated the absorption signal will disappear, and the transfer or exchange of these protons with those at site B will affect the relative populations of the spin states at site B. The net absorption at the second site, B, does not reduce to zero because the relative population differences tend to be restored to thermal equilibrium by the spin-lattice relaxation. The change in absorption at site B can be followed by measuring the intensity of the signal using a weak rf field. Instantaneous saturation of the protons at A will decrease the intensity of the absorption signal of the protons at B to a low, non-zero value as long as the exchange rate between the two sites approximates to the

spin-lattice relaxation time. The useful range of this method is therefore limited to rate processes too slow for access by the line shape method.

2. Determination of rate constants

In presenting the equations used to determine rate constants it will be convenient to use the magnetization in the conventional z-direction $M_z^A(t)$ for protons at site A at a specified time, t, in the static magnetic field, H_z^o. The magnetization, $M_z^A(t)$, depends on the relative spin populations and is zero when the protons are saturated. The line intensity of the protons at a given site is proportional to the magnetization of the protons at that site. In the absence of any saturating rf field the thermal equilibrium magnetization at site A will be denoted by M_z^A.

Consider the case where the thermal equilibrium populations at site A and site B are equal. The lifetime of a proton at site A, τ_A, will be equal to the lifetime at site B, τ_B. Since the rate constant, k, is the inverse of the lifetime, it will be the same for both sites.

$$k = \frac{1}{\tau_A} = \frac{1}{\tau_B} \qquad 2.40$$

3. Decay of magnetization at site B with saturation of site A

The magnetization at site B, $M_z^B(t)$, after the instantaneous application of a saturating rf field at site A when t = 0 is given by (9)

$$M_z^B(t) = M_z^B\left[\left(\frac{\tau_{1B}}{\tau_B}\right)\exp\left(\frac{-t}{\tau_{1B}}\right) + \frac{\tau_{1B}}{T_{1B}}\right] \qquad 2.41$$

where

$$\frac{1}{\tau_{1B}} = \frac{1}{T_{1B}} + \frac{1}{\tau_B} \qquad 2.42$$

and T_{1B} is the spin-lattice relaxation time, τ_B the average lifetime at site B.

As $t \to \infty$ an equilibrium value is obtained

$$M_z^B(\infty) = M_z^B\left[\frac{\tau_{1B}}{T_{1B}}\right] \qquad 2.43$$

from which the initial magnetization at site B can be found

$$M_z^B = \frac{M_z^B(\infty)\ T_{1B}}{\tau_{1B}} \qquad 2.44$$

Substituting from 2.44 into 2.41 yields

$$M_z^B(t) = M_z^B(\infty)\left(\frac{T_{1B}}{\tau_{1B}}\right)\left[\frac{\tau_{1B}}{\tau_B}\ \exp\left(\frac{-t}{\tau_{1B}}\right) + \frac{\tau_{1B}}{T_{1B}}\right] \qquad 2.45$$

Multiplying through and combining terms

$$M_z^B(t) - M_z^B(\infty) = M_z^B(\infty)\left(\frac{T_{1B}}{\tau_B}\right)\exp\left(\frac{-t}{\tau_{1B}}\right) \qquad 2.46$$

Substituting for $M_z^B(\infty)$ on the right from equation 2.43 and cancelling terms

$$M_z^B(t) - M_z^B(\infty) = M_z^B\left(\frac{\tau_{1B}}{\tau_B}\right)\exp\left(\frac{-t}{\tau_{1B}}\right) \qquad 2.47$$

Taking logarithms

$$\ln\left(M_z^B(t) - M_z^B(\infty)\right) = \ln\left[\frac{M_z^B\tau_{1B}}{\tau_B}\right] + \left[\frac{-t}{\tau_{1B}}\right] \qquad 2.48$$

A plot of the logarithm on the left against time should yield a straight line with slope $\left(-\frac{1}{\tau_{1B}}\right)$. Using this value of the slope and rearranging equation 2.44 to

$$\frac{M_z^B(\infty)}{M_z^B} = \frac{\tau_{1B}}{T_{1B}} \qquad 2.49$$

permits the calculation of the spin-lattice relaxation time. When τ_{1B} and T_{1B} are used in equation 2.42, the rate constant, k, for the exchange between site A and site B is obtained.

4. Recovery of magnetization at site B after removal of saturation at site A

Instantaneous removal of the saturating field at site A is followed by the increase in magnetization at site B to its equilibrium value. The magnetization at site B when t = 0, $M_z^B(0)$, will be the value previously designated by $M_z^B(\infty)$ for saturation. Therefore, at the instant when site A experiences the total removal of the double resonance, one can write

$$M_z^A(0) = 0 \quad \text{and} \quad \frac{M_z^B(0)}{M_z^B} = \frac{\tau_{1B}}{T_{1B}} \tag{2.50}$$

where both $M_z^A(t)$ and $M_z^B(t)$ will increase with time. The expressions for the magnetizations at any time are given by (8)

$$M_z^B(t) = M_z^B + c_1 \exp(-\lambda_1 t) + c_2 \exp(-\lambda_2 t) \tag{2.51}$$

$$M_z^A(t) = M_z^A + c_1 \tau_A \left(\frac{1}{\tau_{1B}} - \lambda_1\right) \exp(-\lambda_1 t) + c_2 \tau_A \left(\frac{1}{\tau_{1B}} - \lambda_2\right) \exp(-\lambda_2 t) \tag{2.52}$$

where the values c_1 and c_2 are determined by the initial saturated condition ($t = 0$)

$$c_1 = M_z^B \left[\frac{\lambda_2 (T_{1B} - \tau_{1B})}{T_{1B}(\lambda_1 - \lambda_2)}\right] \tag{2.53}$$

$$c_2 = M_z^B \left[\frac{\lambda_1 (T_{1B} - \tau_{1B})}{T_{1B}(\lambda_2 - \lambda_1)}\right] \tag{2.54}$$

The values for λ_1 and λ_2 are obtained by solving the determinant

$$\begin{vmatrix} \frac{1}{\tau_{1B}} - \lambda & -\frac{1}{\tau_A} \\ -\frac{1}{\tau_B} & \frac{1}{\tau_{1A}} - \lambda \end{vmatrix} = 0 \tag{2.55}$$

Since the average lifetimes of the spin at the two sites have been

specified to be equivalent, that is, $\tau_A = \tau_B$, all subscripts can, for convenience, refer to site B. The solution under conditions of slow exchange is

$$\lambda_1 = \frac{1}{\tau_{1B}} + \frac{1}{\tau_B} \qquad 2.56$$

$$\lambda_2 = \frac{1}{\tau_{1B}} - \frac{1}{\tau_B} = \frac{1}{T_{1B}} \qquad 2.57$$

If it is assumed, as stated earlier, that $\tau_B \sim T_{1B}$ then $\lambda_1 \sim 3\lambda_2$. This would be the longest average lifetime considered. For all τ_B less than T_{1B}, λ_2 would be small and its contribution in equations 2.51 and 2.52 could be neglected. Furthermore, equations 2.53 and 2.54 predict a smaller c value for a larger λ value, and hence the exponential with the larger λ value will decay to zero quickly, leaving the magnetization as a function of the remaining exponential. For the case where $\lambda_1/\lambda_2 = - c_2/c_1 > 3$, equation 2.51 reduces to

$$M_z^B(t) - M_z^B = c_2 \exp\left(\frac{-t}{T_{1B}}\right) \qquad 2.58$$

Using an average value of $T_{1B} = 13$ seconds places an upper limit of 13 seconds for τ_B or a lower limit on the rate constant of $k = .08\ sec^{-1}$. All rates investigated by this method were above this value. The plot of $\ln\left(M_z^B(t) - M_z^B\right)$ versus time will quickly approximate a straight line where the slope yields the value of T_{1B}.

At increasingly longer average lifetimes (lower temperatures), the exchange becomes sufficiently slow that the ratio, $M_z^B(\infty)/M_z^B$,

approaches unity. Thus the curves become increasingly shallow and the slopes difficult to measure. The recovery term, being a function of two exponential terms, is more difficult to obtain. However, if some value of T_{1B} is assumed, it is possible to calculate τ_B (and k) by using equation 2.49. This method is not desirable where the spin-lattice relaxation time cannot be estimated with a fair degree of accuracy.

D. Determination of Activation Parameters

1. Arrhenius Activation Energy

The Arrhenius equation (25)

$$\ln k = \frac{-Ea}{R}\left(\frac{1}{T}\right) + \ln A \qquad 2.59$$

can be used to obtain the activation energy, Ea, and the frequency factor, A, from the slope and intercept of the plot of the natural logarithm of the rate constant, k, against the reciprocal of the absolute temperature. The usefulness of this method is limited to cases where the activation energy and the frequency factor are independent of temperature.

2. Activation parameters from Absolute Rate Theory

Eyring's equation (26)

$$k = \left(\frac{\kappa k_B}{h}\right) T \exp\left(\frac{-\Delta G^{\neq}}{RT}\right) \qquad 2.60$$

can be used to determine the activation parameters where the rate constant, k, at temperature, $T^{o}K$, is related to the free energy of activation, $\Delta G^{\neq}$. κ is the transmission coefficient which usually is set equal to one (14), but may be set equal to one-half if the potential energy diagram is symmetrical about the transition state (15,16). The Boltzmann constant has the symbol, k_B, h is Planck's constant and R is the ideal gas constant.

When the coalescence temperature is accurately known with its related rate constant, k, the Eyring equation can be employed directly

to calculate the free energy of activation. The error will be due to the error in determining the single-valued T and k.

Often the coalescence temperature cannot be determined with a fair degree of accuracy. Substituting from the thermodynamic expression relating the free energy of activation, $\Delta G^{\neq}$, to the enthalpy, $\Delta H^{\neq}$, and entropy, $\Delta S^{\neq}$, of activation

$$\Delta G^{\neq} = \Delta H^{\neq} - T\Delta S^{\neq} \qquad 2.61$$

for $\Delta G^{\neq}$ in equation 2.60, rearranging and taking logarithms of both sides yields

$$\ln\left(\frac{k}{T}\right) = \ln\left[\frac{\kappa k_B}{h}\right] + \left(\frac{-\Delta H^{\neq}}{RT}\right) + \frac{\Delta S^{\neq}}{R} \qquad 2.62$$

A plot of ln (k/T) against (1/T) should yield the enthalpy, $\Delta H^{\neq}$, from the slope and the entropy of activation, $\Delta S^{\neq}$, from the intercept. Then $\Delta G^{\neq}$ could be calculated for the temperature in question using equation 2.61. It assumes, as does the Arrhenius theory, that the forward and reverse reaction rates proceed along the same path, which is a reasonable assumption for restricted rotation studies.

If this is not the case, the ratio of the rate constants can be calculated from the populations of the two sites by the equation

$$k_{AB}P_A = k_{BA}P_B \qquad 2.63$$

where k_{AB} is the rate constant for the transition from A to B, P_A is the population of site A, k_{BA} is the exchange rate constant in going from B to A, and P_B is the population of site B. Knowing the relative

populations of the two sites permits calculation of the activation parameters in both directions.

III. EXPERIMENTAL

A. Sample Preparation

The sample of α,α,α',α',3,4,6-heptachloro-ortho-xylene (HCOX) was used as received from Dr. V. Marks of Hooker Chemical Corporation. A 5 mole % solution in methylcyclohexane included hexamethyldisilane (HMDS) as an internal lock and methylene chloride as an internal standard. The sample was degassed by the freeze-pump-thaw technique before being sealed. The sample tube was heated in a paraffin bath to 100°C to check whether it could withstand the vapor pressure without bursting.

B. The High Resolution Spectra

All of the spectra were obtained from a Varian HA-100D nuclear magnetic resonance spectrometer operating in the frequency sweep mode. The internal lock used was hexamethyldisilane (HMDS). Frequency calibrations were obtained using the period averaging technique and peak positions were assigned assuming that the change in frequency was linearly proportional to distance between calibration points for up to 20 Hz separation. Each spectrum was normally recorded three times with some, at temperatures near coalescence, recorded up to eight times.

The temperature of the sample was regulated by using the V-4341/V-6057 variable temperature accessory and was determined with an iron-constantan thermocouple placed in a toluene sample in the probe. Sufficient time elapsed so that the millivolt output did not drift for at least five minutes. These temperatures were taken both before and after the spectra were obtained. Sufficient time (approximately 30 minutes) was allowed for equilibration of the sample after insertion into the probe and the spectrometer resolution was optimized before each spectrum was run. Effective T_2 values were obtained from half-height linewidth of methylene chloride at each temperature. Spectra were recorded at about $5^{o}C$ intervals, limited at the lower temperature by the slow exchange rate and at the higher temperature by the boiling point of the solvent. The spectra were recorded at a frequency sweep rate of .05 Hz/sec.

C. Double Resonance Saturation Transfer

A Hewlett-Packard audio oscillator, model 4204A, was used in the double resonance saturation transfer experiment. The HA-100 was connected to a flat-bed recorder with the controls set in such a way that it indicated the peak height while "sitting" on it. Great care was taken not to saturate the signal with the rf field at the observing frequency. In addition, the observing and saturating frequencies were adjusted by trial and error to compensate for the shift in peak positions that occurred with the large saturating field. Both decay and recovery times were recorded and at least six trials were made at each temperature.

IV. RESULTS AND DISCUSSION

A. General Appearance of the Spectra at Various Temperatures

Earlier studies (27,28,29) have reported the stable conformers of α,α-dihalotoluene derivatives to be those in which the side chain protons lie in the plane of the aromatic ring. Similar findings have been reported for the analogous derivatives of meta- (30) and para- (31) xylenes and mesitylene (32) compounds. This study deals specifically with α,α,α',α',3,4,6-heptachloro-ortho-xylene (HCOX). Due to the proximity of the two substituted methyl groups to each other, steric considerations are of greater consequence than in the previous investigations. Such steric considerations (33) indicate that the rotation of the two methyl groups is synchronized and in opposite directions, suggesting only two conformers with roughly equal populations.

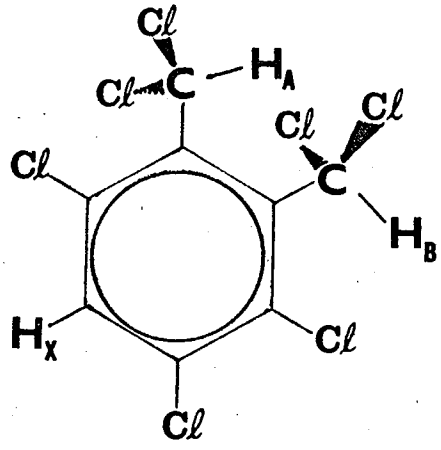

I

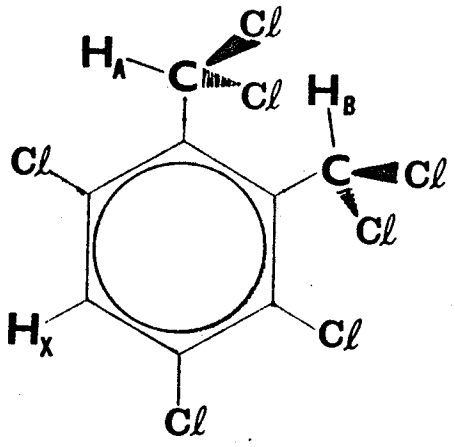

II

Figure 1

The two stable conformers of α,α,α',α',3,4,6-heptachloro-ortho-xylene (HCOX).

These conformations are related by a concerted 180^{o} rotation, but in opposite directions, of the two side chain groups about their respective C-C bonds. Such a rotation effectively changes the magnetic environment of all three protons. At lower temperatures, where the lifetime of each conformer is relatively long, the spectrum consists of the superpositioning of the peaks corresponding to the two conformers as shown in Figure 2a. Increasing the temperature shortens the lifetime and the conformers interconvert more rapidly causing the observed peaks to broaden until they merge together to form an average signal. A further increase in the rate of exchange decreases the width of this averaged peak to its limiting value due mainly to the magnetic field inhomogeneity (approximately 0.2 Hz). The peaks assigned to the aromatic protons coalesced at lowest temperature, but it was not possible to determine which of the methine proton peaks coalesced first or whether all four peaks coalesced at the same temperature.

Due to limitations of the methylcyclohexane used as solvent, with a boiling point of $100.9^{o}C$ (34), the maximum temperature of measurement was restricted to $98^{o}C$, insufficiently high to yield the resolved three-peak fast exchange spectra.

The representative spectra of a 5 mole % solution of HCOX in methylcyclohexane at various temperatures are shown with the corresponding simulated spectra in section D.

B. Conformational Assignment

At ambient temperature, 305°K, the spectrum contained six relatively well-resolved peaks (Figure 2) as expected for the slow exchange region. However, the rate of exchange between the two conformers was still sufficiently rapid so that a saturation transfer technique (23) could be employed in the assignment of the peaks of Figure 2, numbered from low field to high field.

Saturation of peak 1 caused the disappearance of peak 3; peaks 4, 5 and 6 remain unaffected. The transfer of saturation permitted the assignment of peaks 1 and 3 to the same proton in the two conformers. Saturation of peak 2 caused peaks 3 and 6 to be noticeably reduced in intensity; peaks 4 and 5 were relatively unaffected. The reduction in the intensity of peak 3 is rationalized as due to the partial saturation of peak 1. Peaks 2 and 6 were assigned to the second proton in the two conformers. By deduction, the third proton in the two conformers should have been assigned to peaks 4 and 5. This assignment was confirmed by saturating peaks 3 and 4; peaks 2 and 6 remained relatively unchanged and peaks 1 and 5 were significantly reduced in intensity.

By inspection of Figure 1, H_A and H_X of conformer I should display spin-spin coupling according to the "zig-zag" rule (35). Peaks 2 and 4 were both split, and hence were assigned to I. In keeping with earlier assignments of analogous compounds (27,36) the downfield peak, 2, was assigned to the methine proton, $H_{A(I)}$, and the upfield peak was assigned to the ring proton of conformer I, $H_{X(I)}$. This entailed that peak 6 arose from the resonance of $H_{A(II)}$ and peak 5 from $H_{X(II)}$.

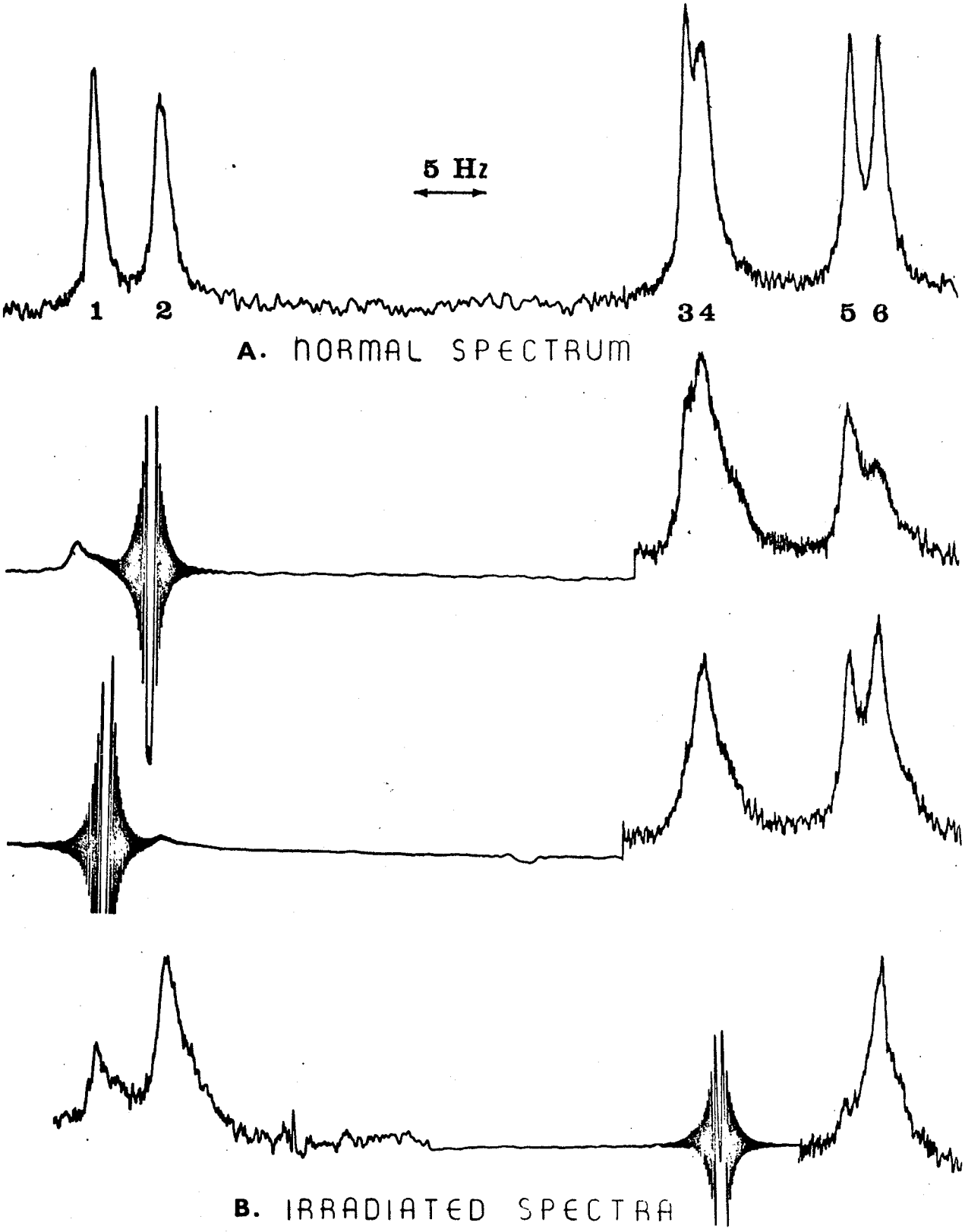
5 Hz
1
2
3 4
5 6
A. NORMAL SPECTRUM
B. IRRADIATED SPECTRA

Peak 1 was assigned to conformer II as the environment of $H_{B(II)}$ is most like that of $H_{A(I)}$. Peak 3 must then arise from the resonance of $H_{B(I)}$. The complete assignment is shown in Figure 3A.

Since this assignment does not agree with previous reports (37) (see Figure 3B), a second method involving steric crowding, as reported by Peeling, et al. (32) was also applied. The results agreed with the above assignment for the methine protons. To assign the aromatic ring protons required consideration of neighbouring atoms "twice removed" (32). When this was done the relative positions of all pairs of peaks agreed with the above; the $H_{A(II)}$ and $H_{B(I)}$ peaks are farthest downfield, the $H_{x(I)}$ and $H_{A(I)}$ peaks are farthest upfield, while the $H_{B(II)}$ and $H_{x(II)}$ peaks occur at intermediate fields. Long range coupling permits unambiguous assignment, as before, for $H_{B(I)}$, $H_{x(I)}$, $H_{B(II)}$ and $H_{A(I)}$ but there appears to be no intuitive way to differentiate between $H_{x(II)}$ and $H_{A(II)}$ when using this method.

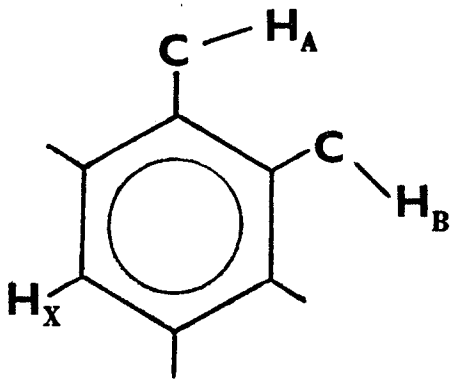

I

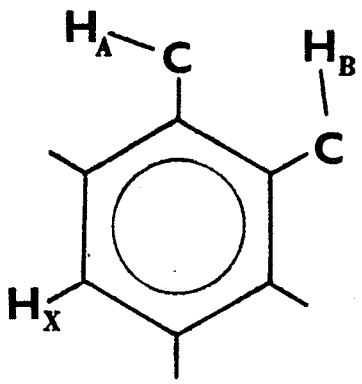

II

A in methylcyclohexane

B in tetradecane

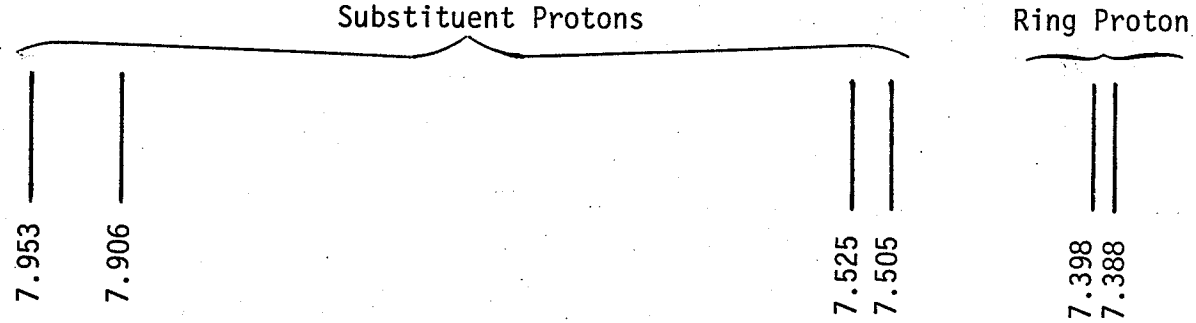

C. Relative Populations of the Two Conformers

The peaks assigned to the two conformers were sufficiently dispersed for a determination of the relative populations by measuring the areas under the peaks. The spectra were photocopied and the average weight of the peaks assigned to each conformer was used in the determination. The data in Table 1 indicates that the populations of the two conformers were the same to within the experimental error at the five temperatures investigated.

The temperatures reported were assumed representative of the temperature range used in the study and that therefore the population difference of the two conformers could be ignored over the entire range used in line shape analysis.

Table 1

Relative intensities of the three peaks of I and II in the low temperature region.

Temperature (^{o}C)	Ratio* I/II
-60	0.99 ± .06**
-20	1.00 ± .04
17.3	1.02 ± .04
20	0.98 ± .02
25.7	0.98 ± .02

* The ratios given here were determined by weighing.

** The errors quoted here are standard deviations.

D. Determination of Rate Constants

1. From line shape analysis

Rate constants for the region of intermediate lifetimes were obtained by comparison of the line shapes of experimental spectra with those generated by the computer program DNMR2 (Dynamic Nuclear Magnetic Resonance - Second Edition) (10). This program is essentially the same as DNMR, for which the program (38) and the theory (11) have been described elsewhere. DNMR2 is designed to compute complex exchange broadened spectra which can be graphically displayed on a Calcomp plotter. The algorithm is based on a quantum mechanical theory of exchange effects on the line shapes of high resolution nuclear magnetic resonance spectra. The data generated and plotted requires chemical shifts, coupling constants, relaxation times, relative populations, and certain scaling parameters as input.

Relative populations have been discussed in section C. Scaling parameters were determined from the experimental spectra. Effective spin-spin relaxation times were estimated from the line shape of the methylene chloride proton resonance peak at each temperature; T_2 values varied between 1.4 and 1.6 seconds. The coupling constant between the methine proton, $H_{A(I)}$, and the ring proton, $H_{X(I)}$, was measured directly at lower temperatures; $J_{H(x)H(A)} = 0.45$ Hz with all other coupling constants set equal to zero.

The observed peak centres, as obtained for all temperatures investigated, are recorded in Table 2. The observed chemical shifts

in Hz were plotted against temperature (^{o}C) in Figure 4 and against the reciprocal of the absolute temperature (K^{-1}) in Figure 5. The initial chemical shifts used in the calculations were obtained from the former graph. Although the agreement between the simulated and observed spectra was excellent, it was found necessary to change the estimated value of the chemical shift by a few tenths of a hertz by reference to Figure 5 in order to obtain the best fit between the calculated and the experimental spectrum. A series of rate constants was entered to obtain a set of computer-simulated spectra. A visual match between a calculated spectrum and an observed one was the only requirement for accepting a rate constant as valid. The estimated error is included with the rate constants in Table 4.

Experimental spectra, together with the matched calculated spectra, are presented in Figures 6 to 21.

Table 2

Observed peak centres in Hz downfield from HMDS for HCOX in methylcyclohexane at various temperatures.

Temp. (^{o}C)	Observed Chemical Shift (Hz)					
	1	2	3	4	5	6
-60.0	792.8	788.2	755.8	755.8	745.4	742.5
-20.0	795.0	789.7	755.1	754.8	745.6	742.8
0.0	794.22	789.72	755.16	754.9	745.15	742.80
5.0	794.37	789.82	755.26	754.96	745.0	742.7
17.3	794.61	790.11	755.43	754.75	745.18	742.98
20.0	794.64	790.16	755.38	754.70	745.07	742.95
25.7	794.75	790.28	755.44	754.57	745.00	742.96
27.7	794.83	790.31	755.47	754.58	745.04	743.03
32.8	794.70	790.27	755.33	754.44	744.79	742.94
36.5	794.96	790.43	755.35	754.34	744.77	743.00
41.1	795.00	790.54	755.42	754.25	744.79	743.06
45.1	795.07	790.59	755.34	754.25	743.92	

Table 2 continued

47.4	795.07		790.63	754.64	743.91
50.8	795.19		790.58	754.48	744.07
54.1	795.19		790.75	754.34	744.18
58.9	795.19		790.51	753.65	744.48
63.4		791.94		757.18	748.19
69.1		792.00			
74.5		789.46			
79.5					
83.2		~778			
90.0		~773			
95.9					
98.0					

749.05
748.82
748.68
748.60
748.40
748.40
747.87

Figure 4

Observed peak centres for a 5 mole % solution of HCOX in methylcyclohexane plotted against temperature (^{o}C). Data from Table 2.

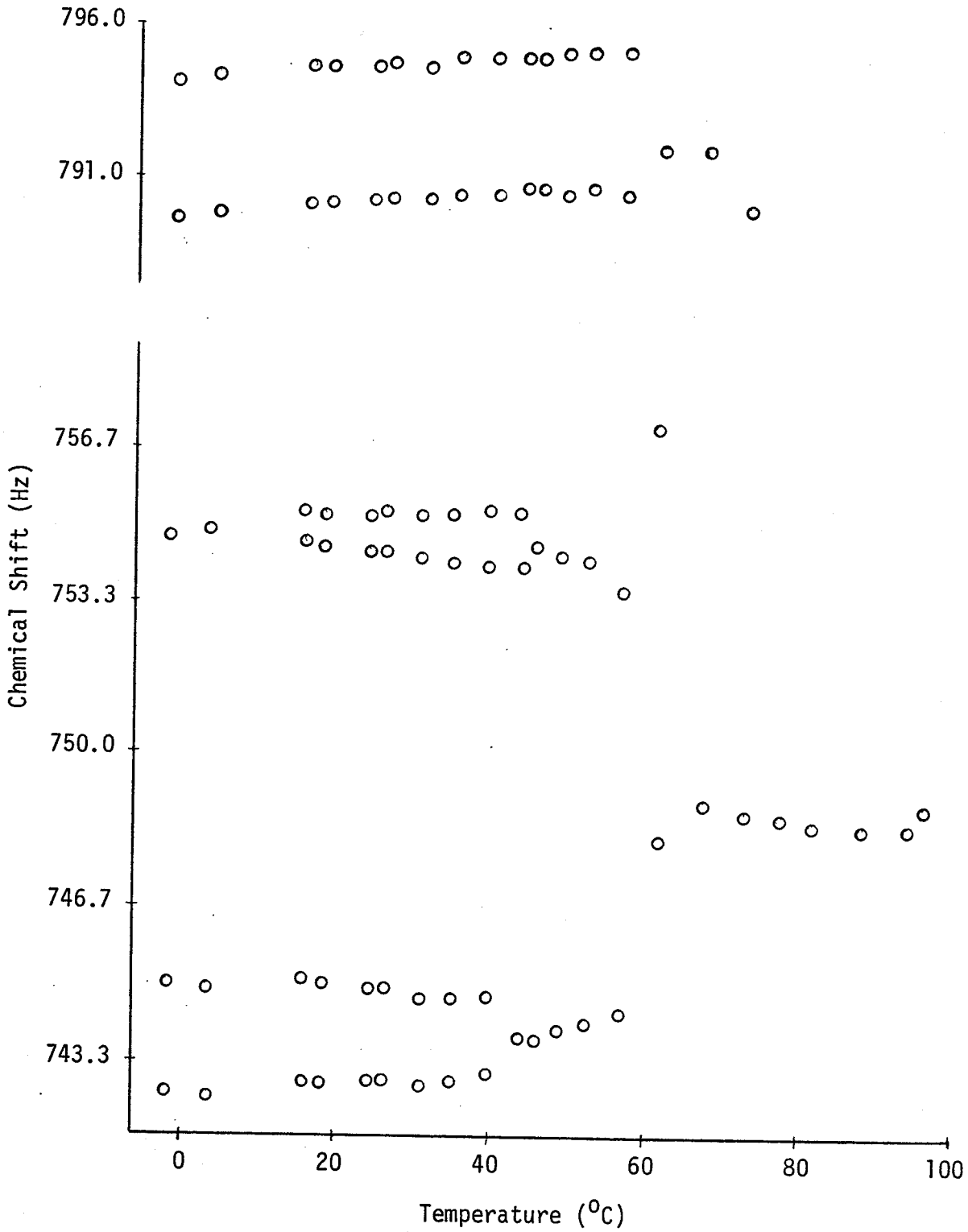
796.0
791.0
756.7
753.3
750.0
746.7
743.3
Chemical Shift (Hz)
0
20
40
60
80
100
Temperature (°C)

Figure 5

Observed peak centres for a 5 mole % solution of HCOX in methylcyclohexane plotted against the reciprocal of the absolute temperature. Data from Table 2.

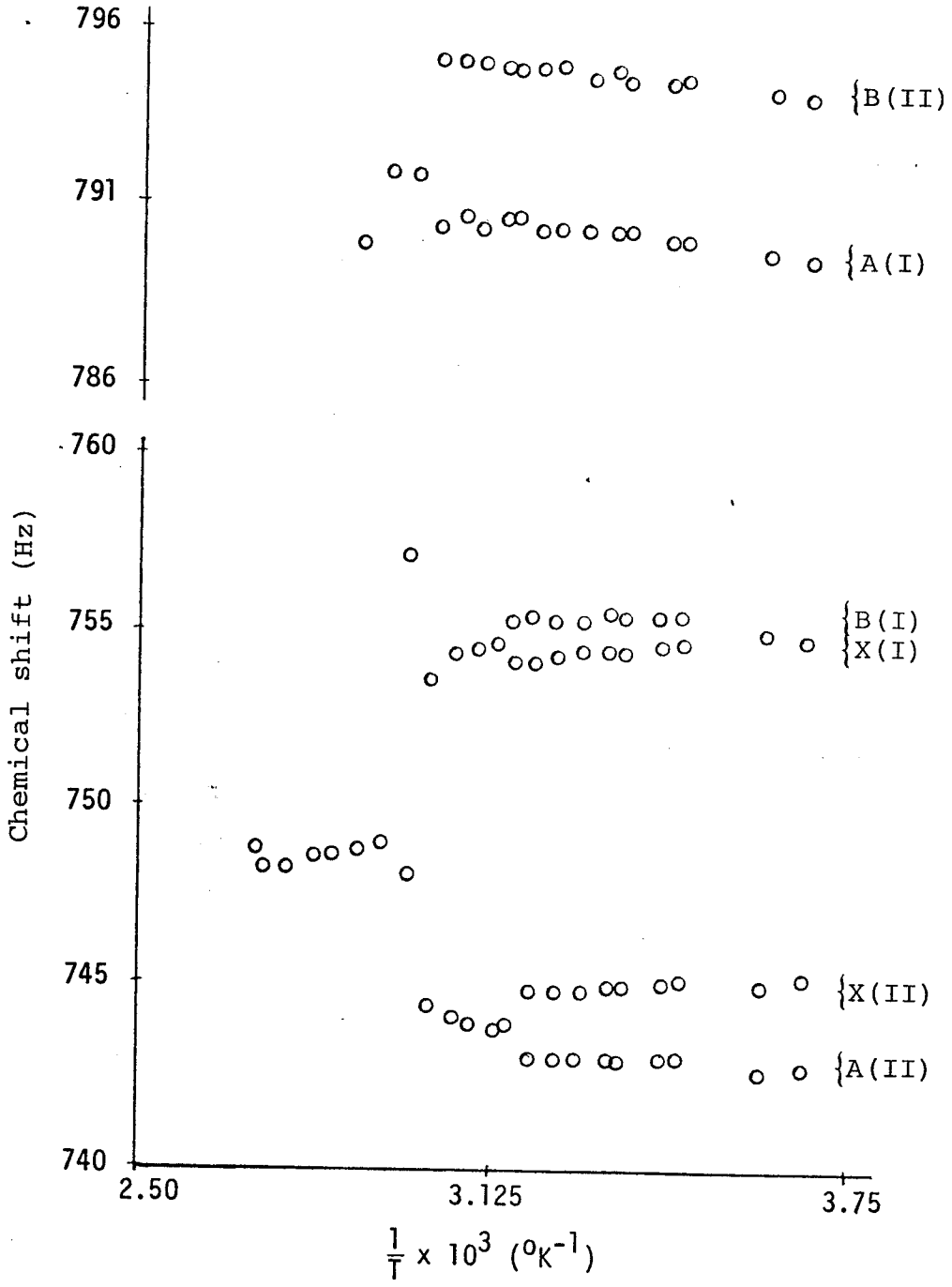
796
791
786
760
755
750
745
740
Chemical shift (Hz)
B(II)
A(I)
B(I)
X(I)
X(II)
A(II)
2.50
3.125
3.75
1/T x 10^3 (°K^-1)

Figure 6

Experimental and calculated N.M.R. spectra of a 5 mole % solution of HCOX in methylcyclohexane at $300.9^{o}K$. $k = 1.1\ sec^{-1}$.

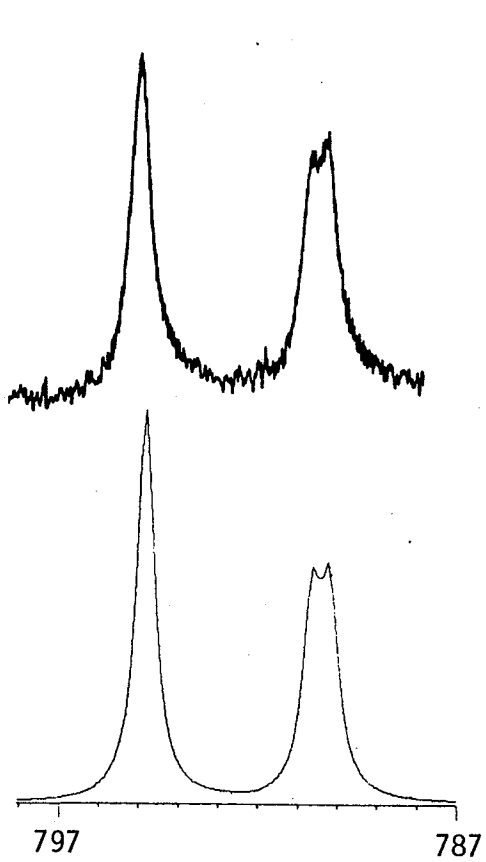
797
787

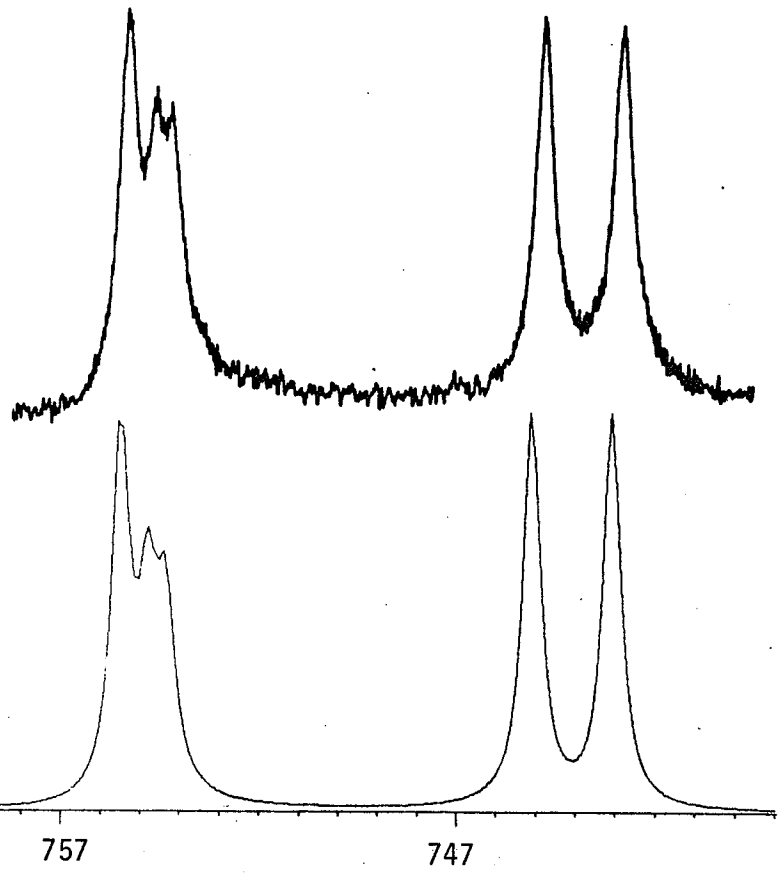
757
747

Figure 7

Experimental and calculated N.M.R. spectra of a 5 mole % solution of HCOX in methylcyclohexane at $305.8^{o}K$. $k = 2.60\ sec^{-1}$.

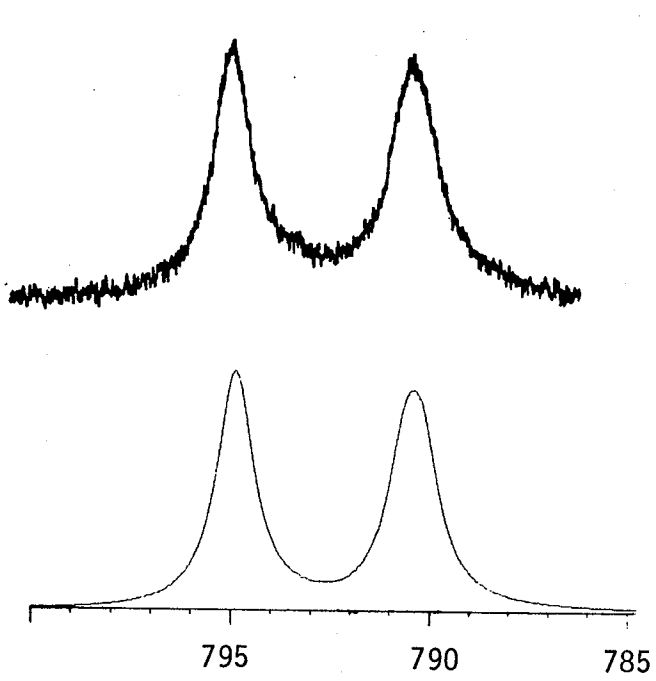
795
790
785

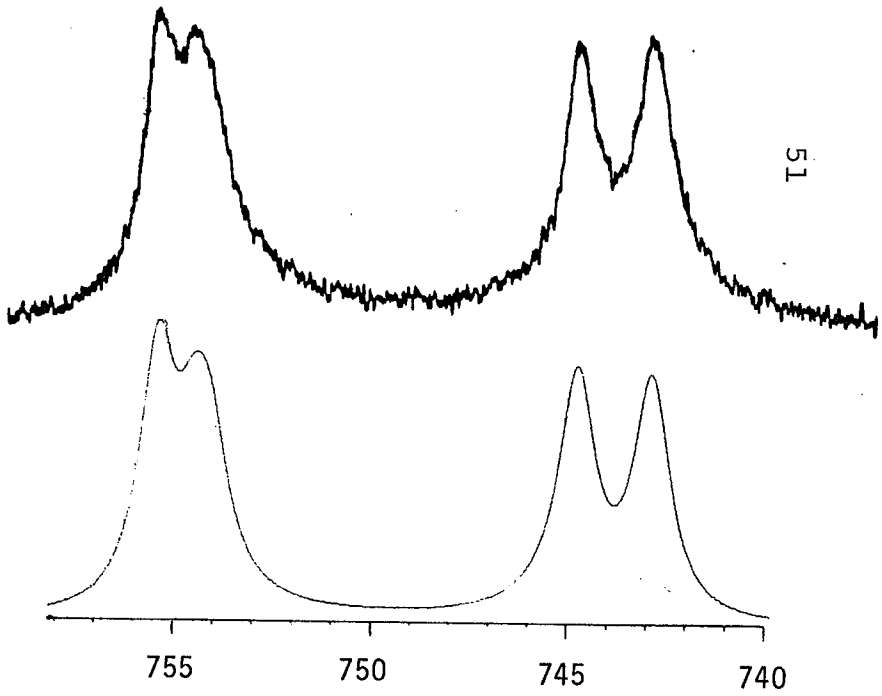
755
750
745
740

Figure 8

Experimental and calculated N.M.R. spectra of a 5 mole % solution of HCOX in methylcyclohexane at $309.5^{o}K$. $k = 3.50\ sec^{-1}$.

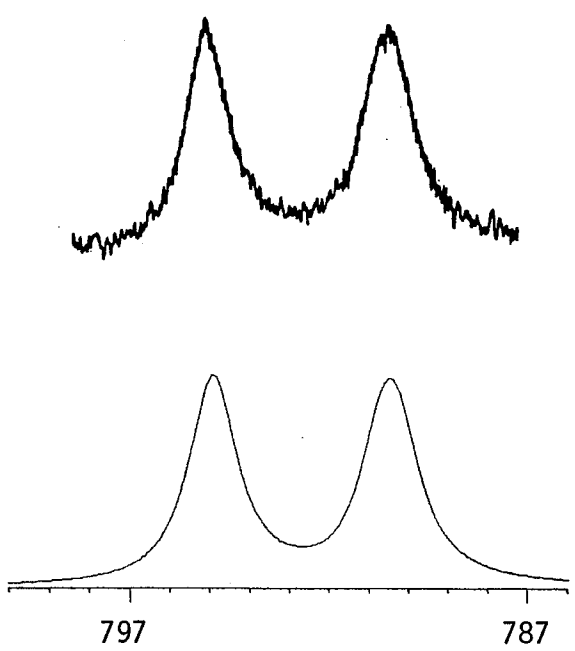
797
787

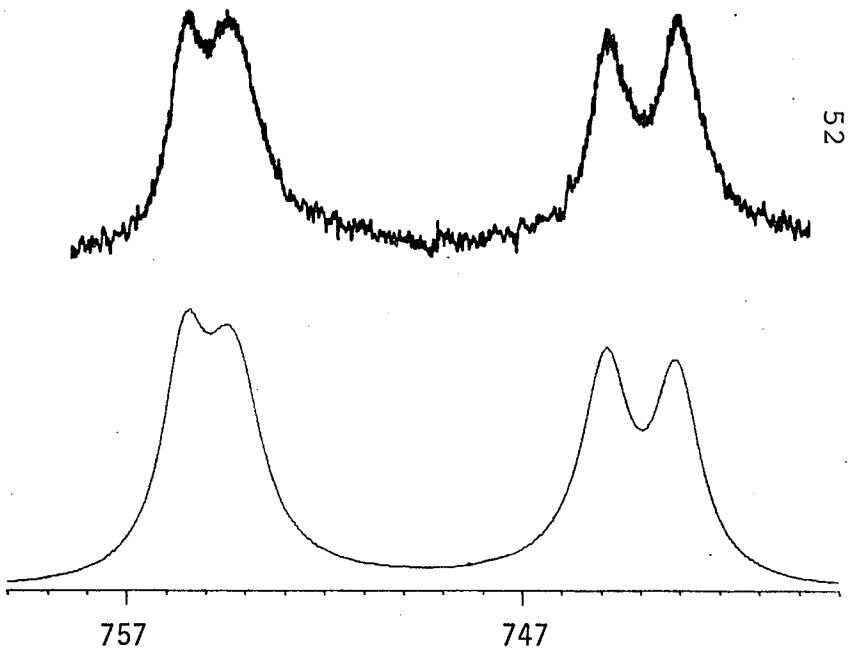
757
747

Figure 9

Experimental and calculated N.M.R. spectra of a 5 mole % solution of HCOX in methylcyclohexane at 314.1^{o}K. k = 4.2 sec^{-1}.

797
787
757
747
737

Figure 10

Experimental and calculated N.M.R. spectra of a 5 mole % solution of HCOX in methylcyclohexane at 318.1^{o}K. k = 6.6 sec^{-1}.

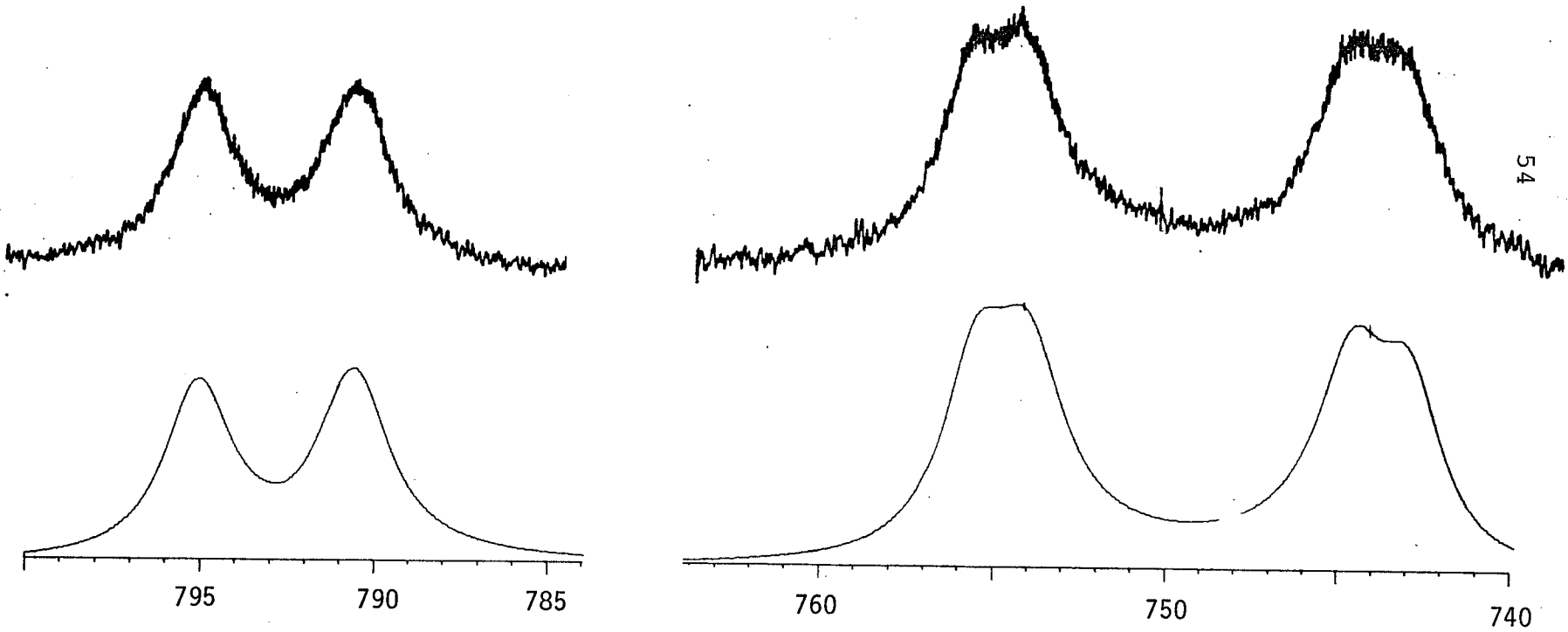
795
790
785
760
750
740

Figure 11

Experimental and calculated N.M.R. spectra of a 5 mole % solution of HCOX in methylcyclohexane at $320.0^{o}K$. $k = 8.0\ sec^{-1}$.

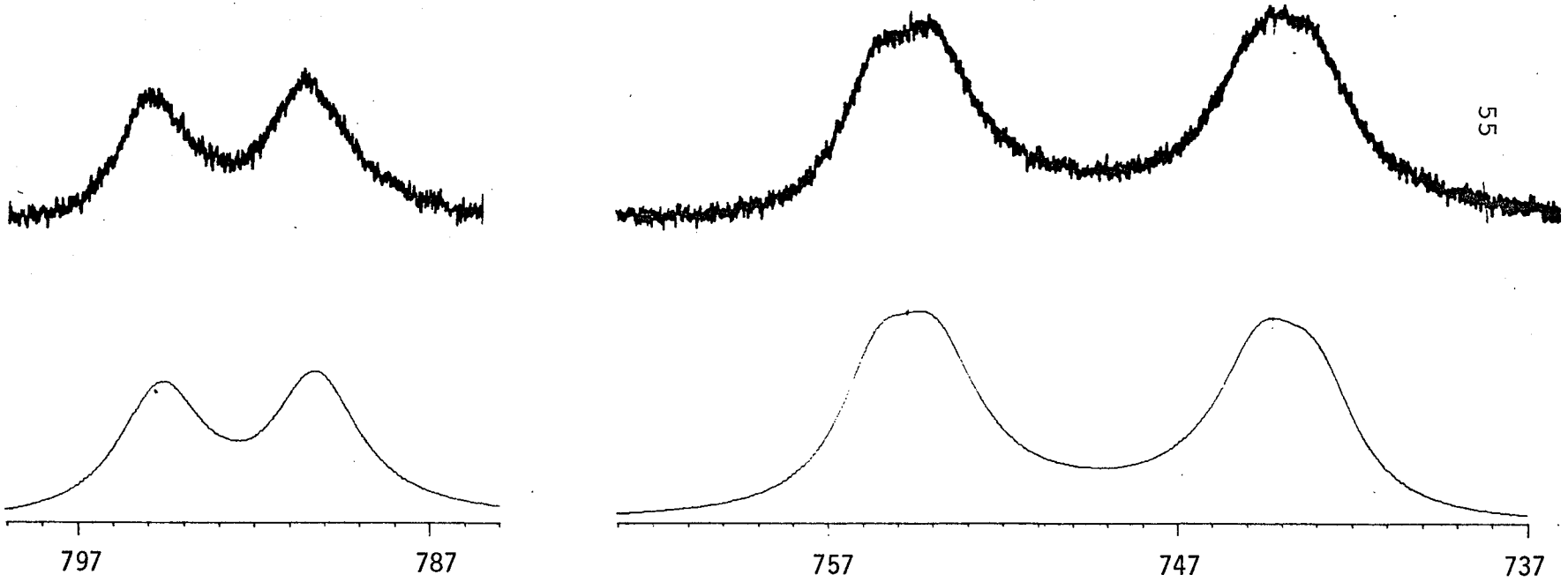
797
787
757
747
737

Figure 12

Experimental and calculated N.M.R. spectra of a 5 mole % solution of HCOX in methylcyclohexane at $323.8^{o}K$. $k = 11.0\ sec^{-1}$.

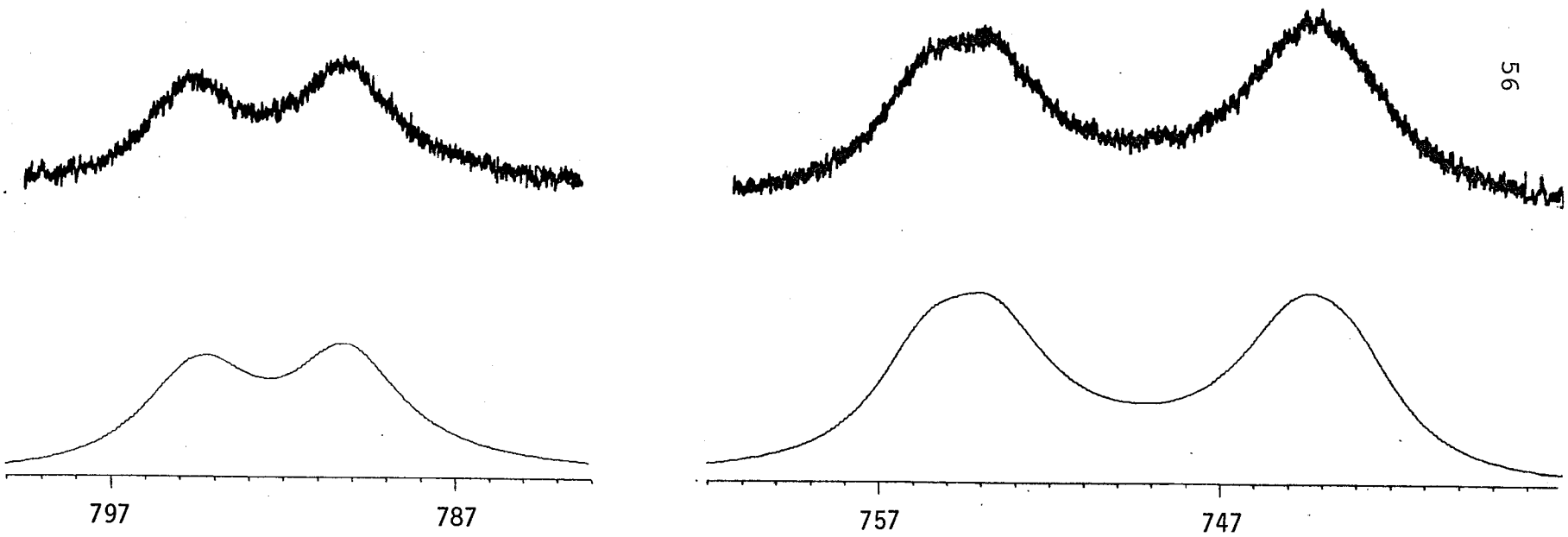
797
787
757
747

Figure 13

Experimental and calculated N.M.R. spectra of a 5 mole % solution of HCOX in methylcyclohexane at $327.1^{o}K$. $k = 12.5\ sec^{-1}$.

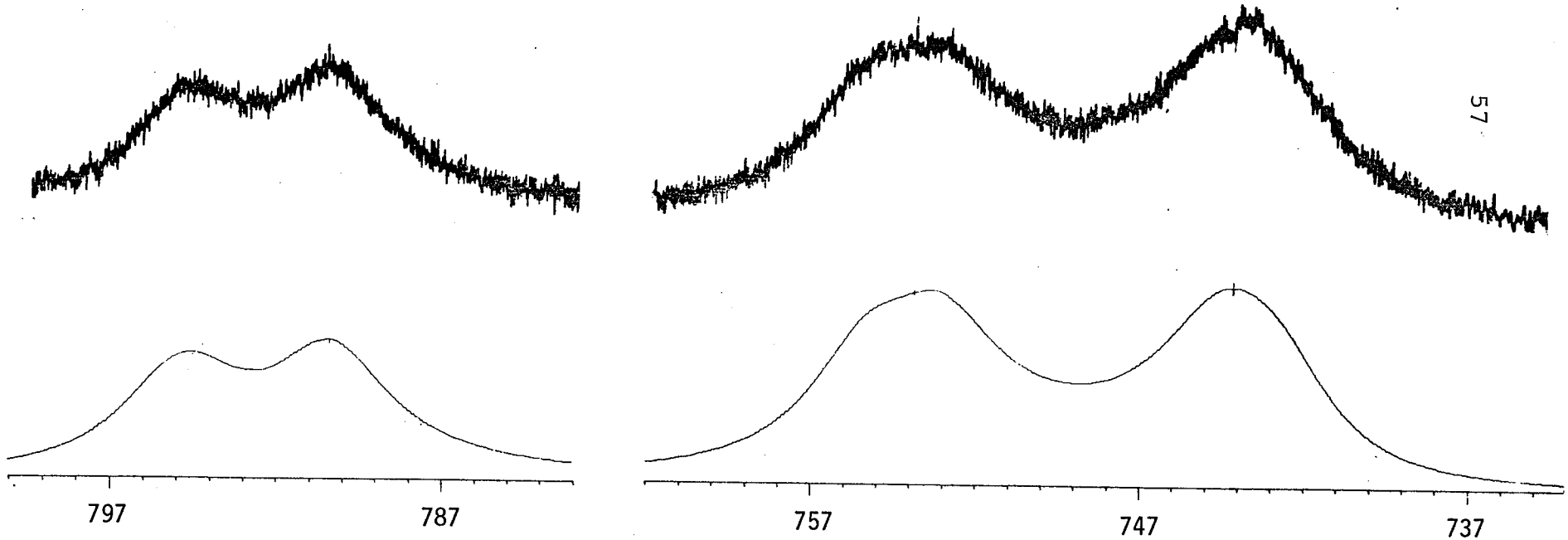
797
787
757
747
737

Figure 14

Experimental and calculated N.M.R. spectra of a 5 mole % solution of HCOX in methylcyclohexane at $331.9^{o}K$. $k = 20.5\ sec^{-1}$.

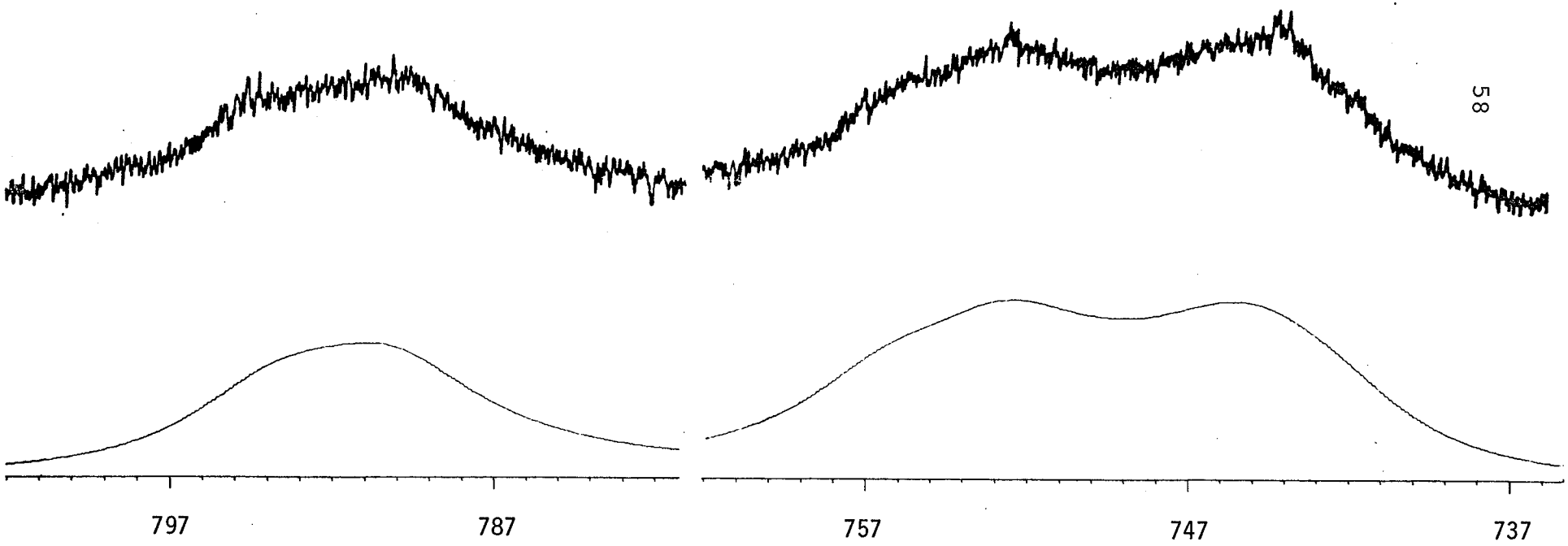
797
787
757
747
737

Figure 15

Experimental and calculated N.M.R. spectra of a 5 mole % solution of HCOX in methylcyclohexane at $336.4^{o}K$. $k = 26.0\ sec^{-1}$.

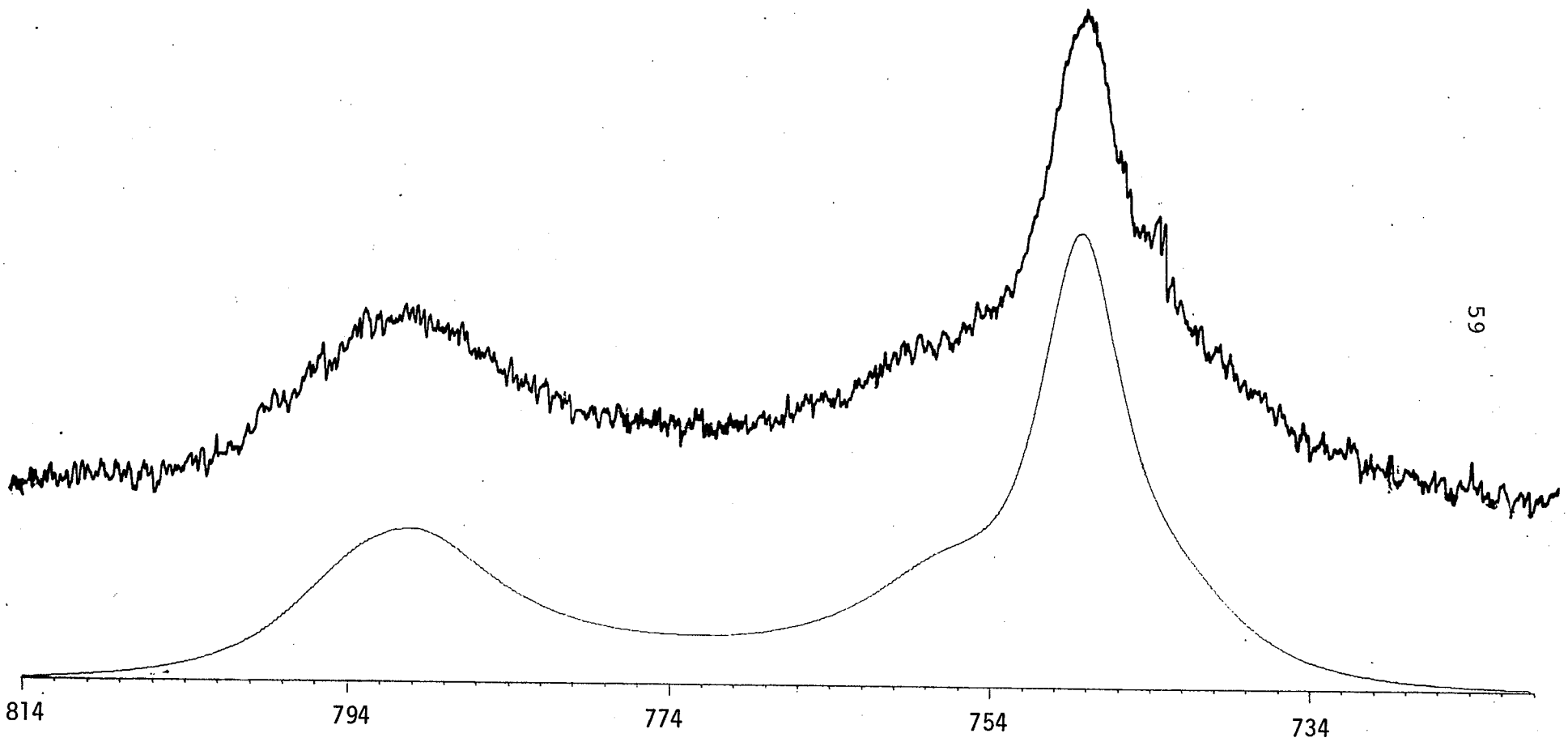
814
794
774
754
734

Figure 16

Experimental and calculated N.M.R. spectra of a 5 mole % solution of HCOX in methylcyclohexane at 342.1^{o}K. k = 36.0 sec^{-1}.

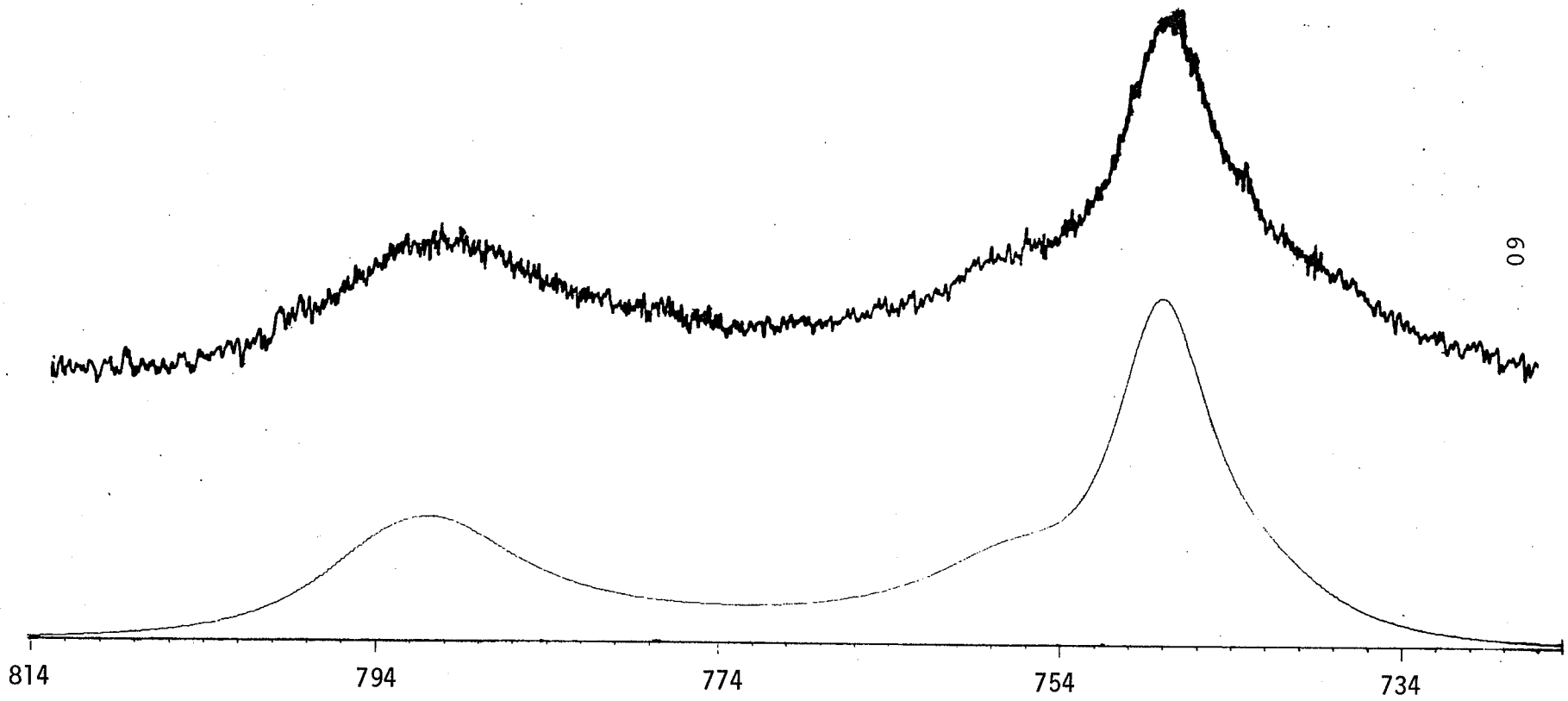
60
814
794
774
754
734

Figure 17

Experimental and calculated N.M.R. spectra of a 5 mole % solution of HCOX in methylcyclohexane at $347.5^{o}K$. $k = 49.0\ sec^{-1}$.

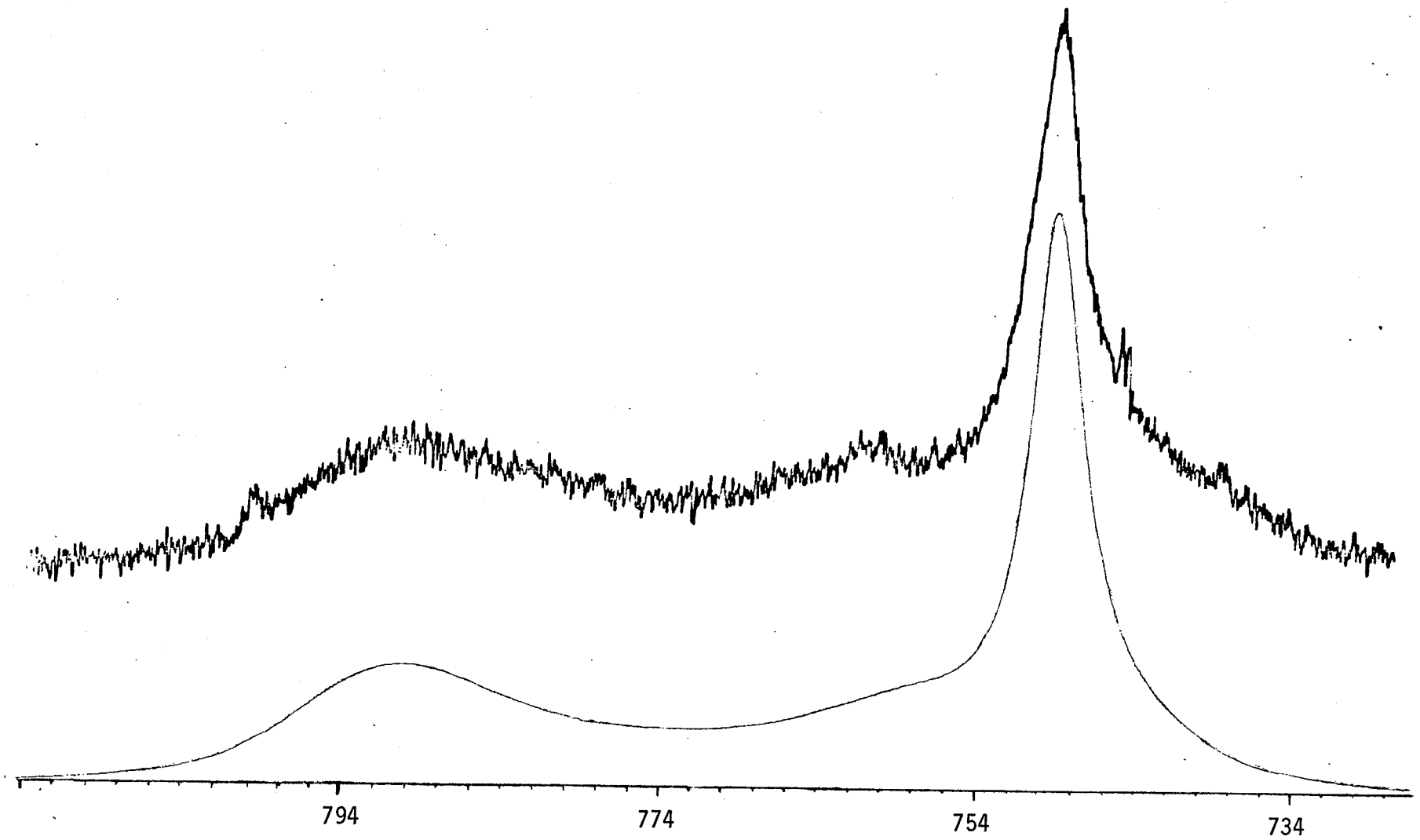
794
774
754
734

Figure 18

Experimental and calculated N.M.R. spectra of a 5 mole % solution of HCOX in methylcyclohexane at $352.5^{o}K$. $k = 72.0\ sec^{-1}$.

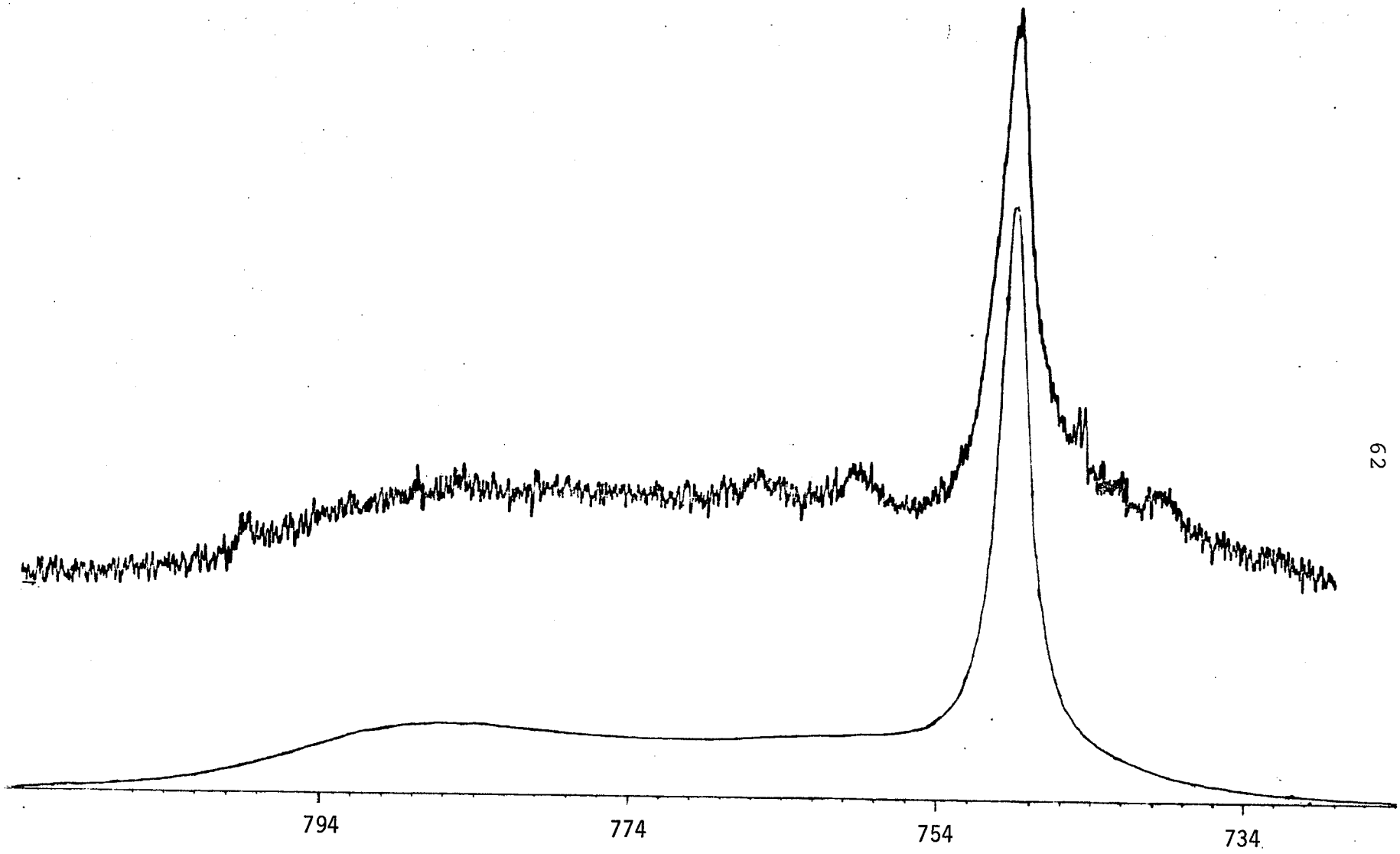
794
774
754
734

Figure 19

Experimental and calculated N.M.R. spectra of a 5 mole % solution of HCOX in methylcyclohexane at $356.2^{o}K$. $k = 104\ sec^{-1}$.

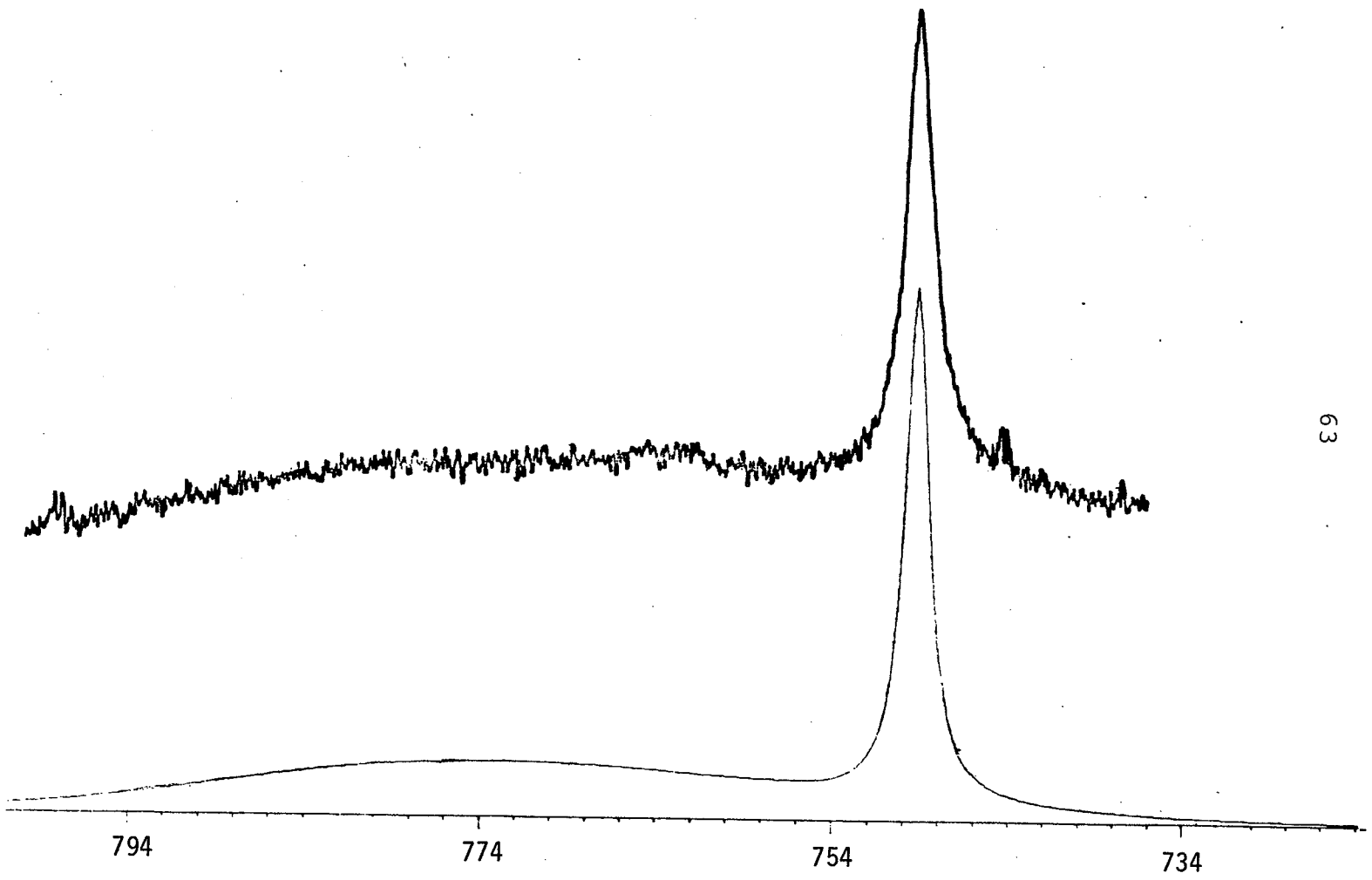
794
774
754
734

Figure 20

Experimental and calculated N.M.R. spectra of a 5 mole % solution of HCOX in methylcyclohexane at $363.0^{o}K$. $k = 160\ sec^{-1}$.

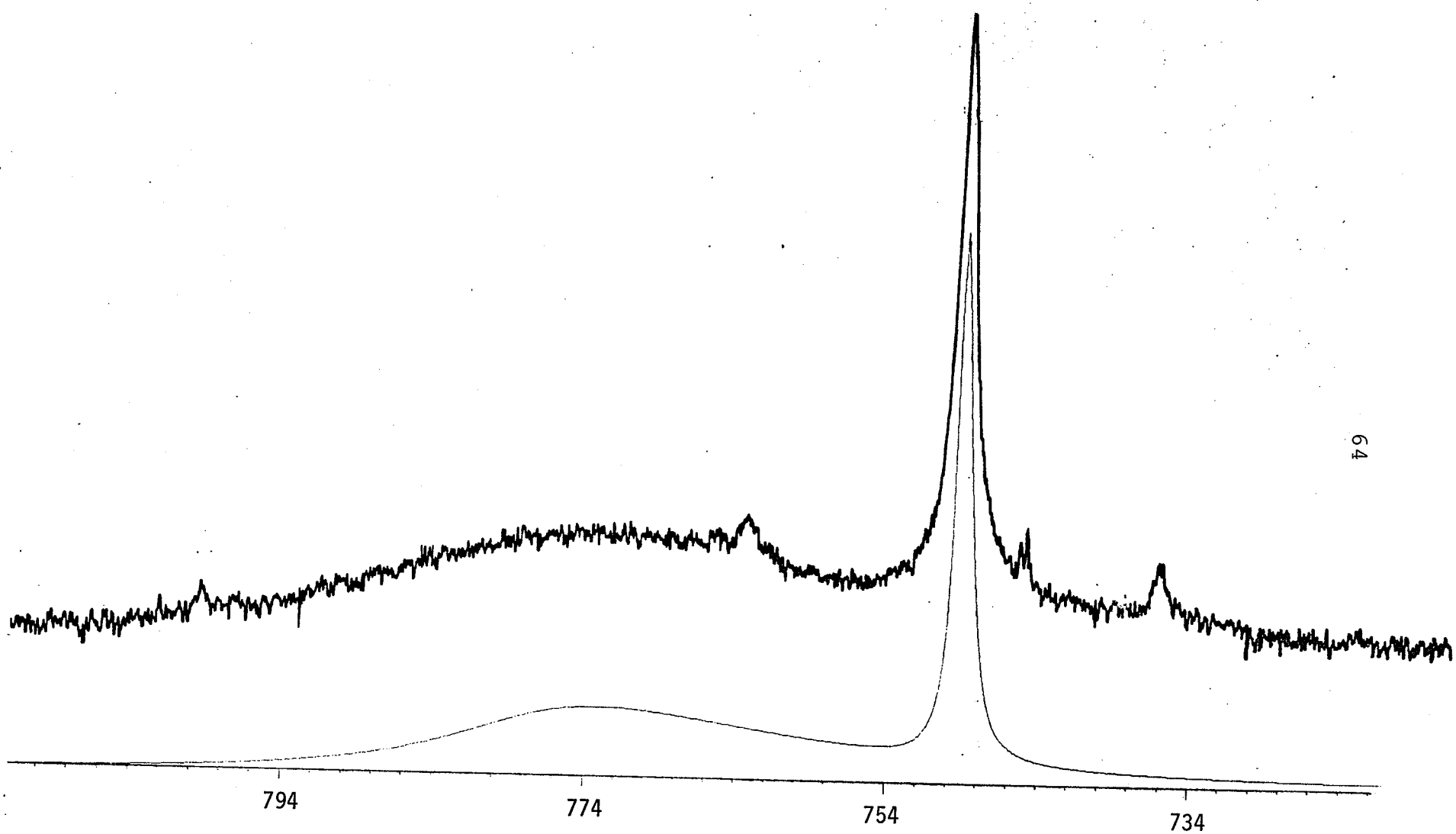
794
774
754
734

Figure 21

Experimental and calculated N.M.R. spectra of a 5 mole % solution of HCOX in methylcyclohexane at $369.0^{o}K$. $k = 198\ sec^{-1}$.

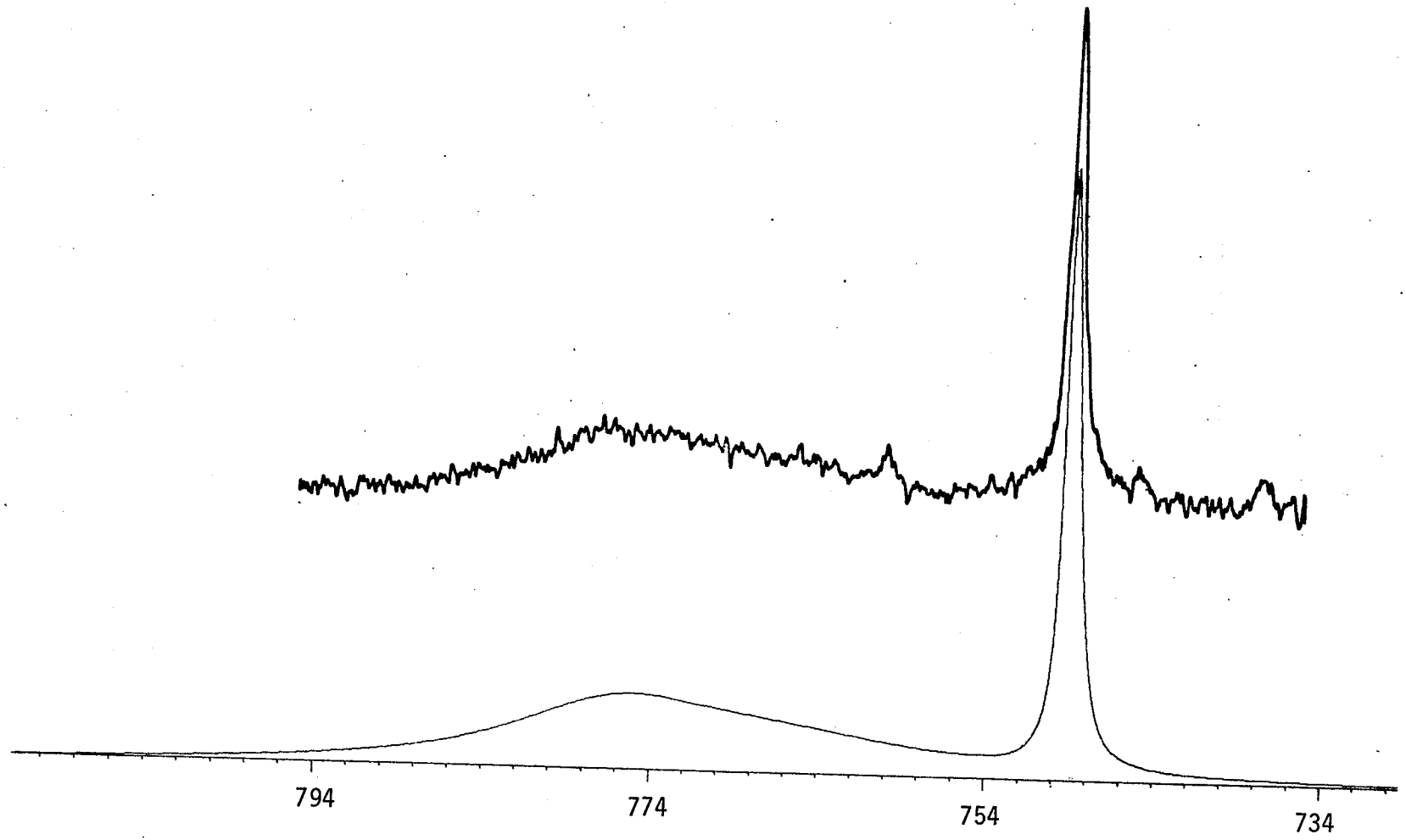
794
774
754
734

2. Using the double resonance saturation transfer technique

At the desired temperature the chemical shifts of one of the protons was measured for each of the two conformers. The proton resonance was saturated at one of the positions while the resonance intensity at the other position was monitored as a function of time. Representative spectra and the plots used to obtain τ_1 and T_1 are shown in Figures 22 to 29. Some trials had to be discarded because of the difficulty in recording intensity changes when the irradiated peak was less than 20 Hz away. At temperatures below $-5^{o}C$ the rate of saturation transfer was too slow to use this method.

The rate constants for each trial were obtained by using equations 2.42 and 2.40.

Figure 22

Double resonance saturation transfer between protons B(II) and B(I) in HCOX at 278.1^{o}K as a function of time. The saturating field is applied to B(I) at t = 0 and is removed at t' = 0.

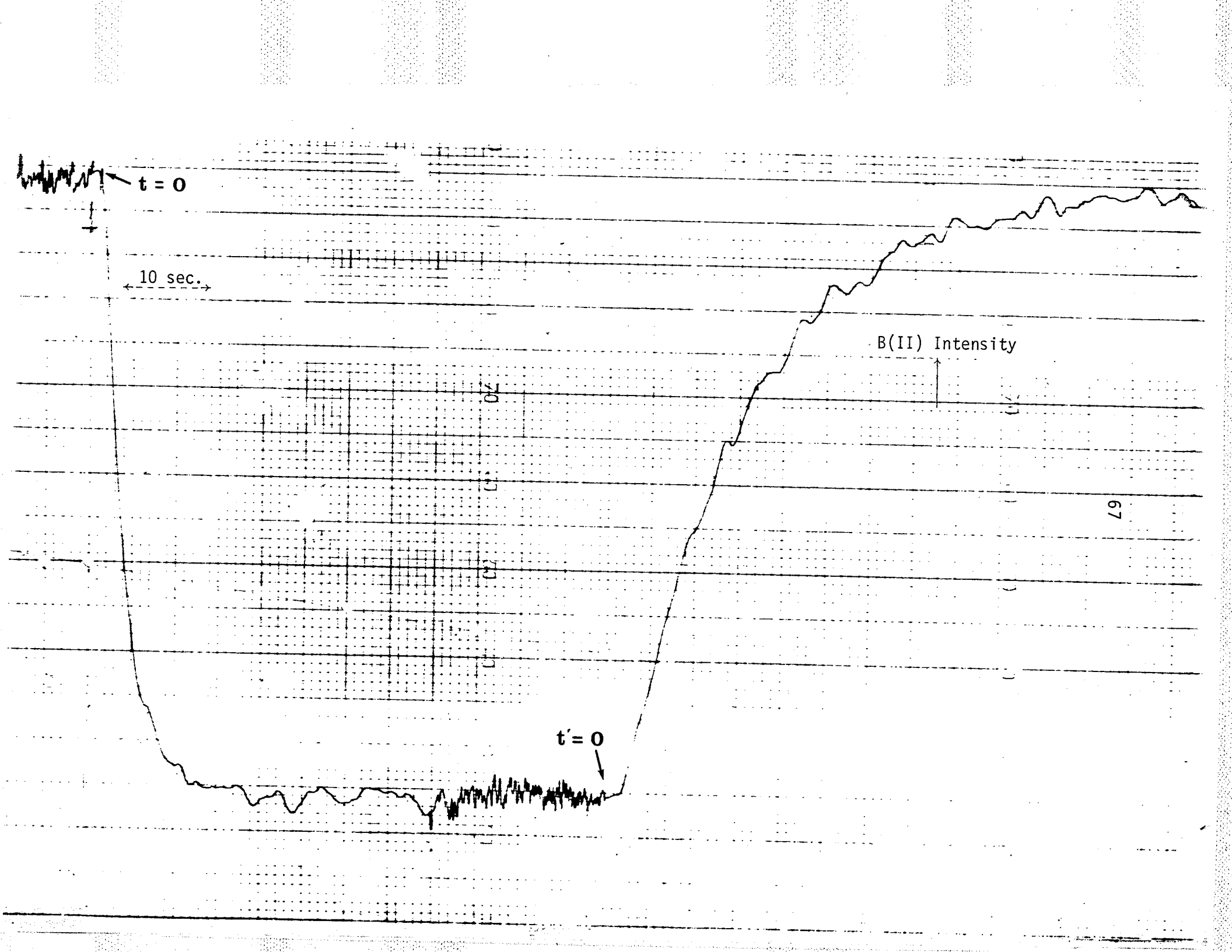
t = 0
10 sec.
B(II) Intensity
t′ = 0

Figure 23

A plot of $\ln \left\{ M_z(t) - M_z(\infty) \right\}$ versus time and of $\ln \left\{ M_z(t) - M_z(0) \right\}$ versus time for the decay and recovery of proton B(II) at 278.1°K. Data obtained from Figure 22. $k = 0.284\ sec^{-1}$.

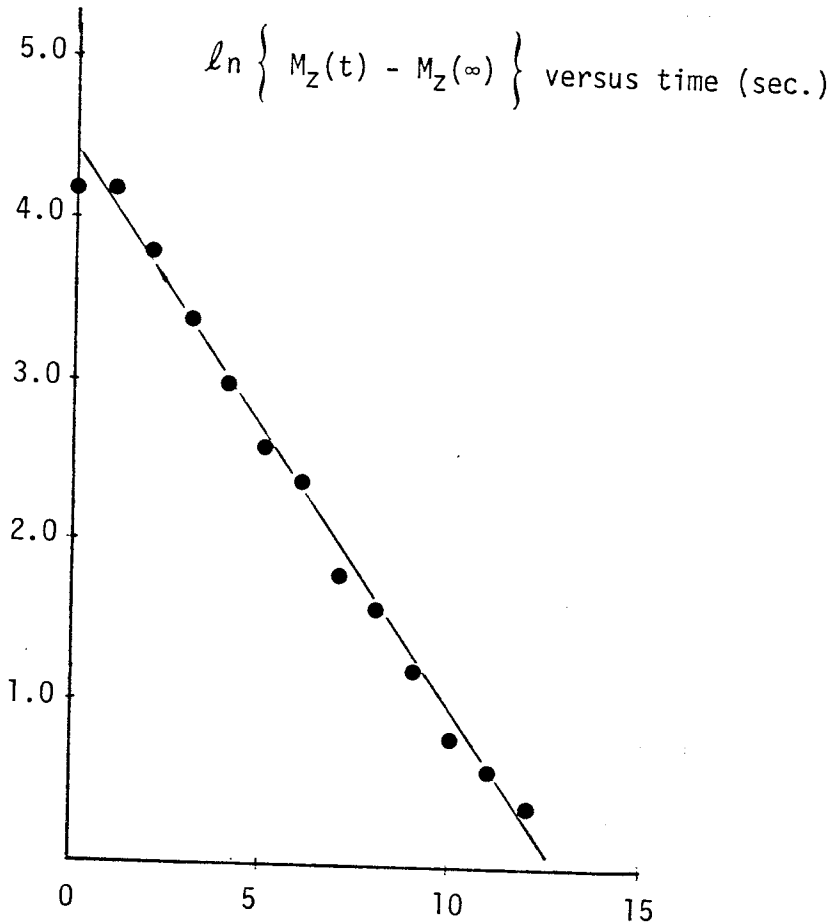

slope: $-0.3541\ sec^{-1}$

τ_1: 2.809 sec.

Decay Curve

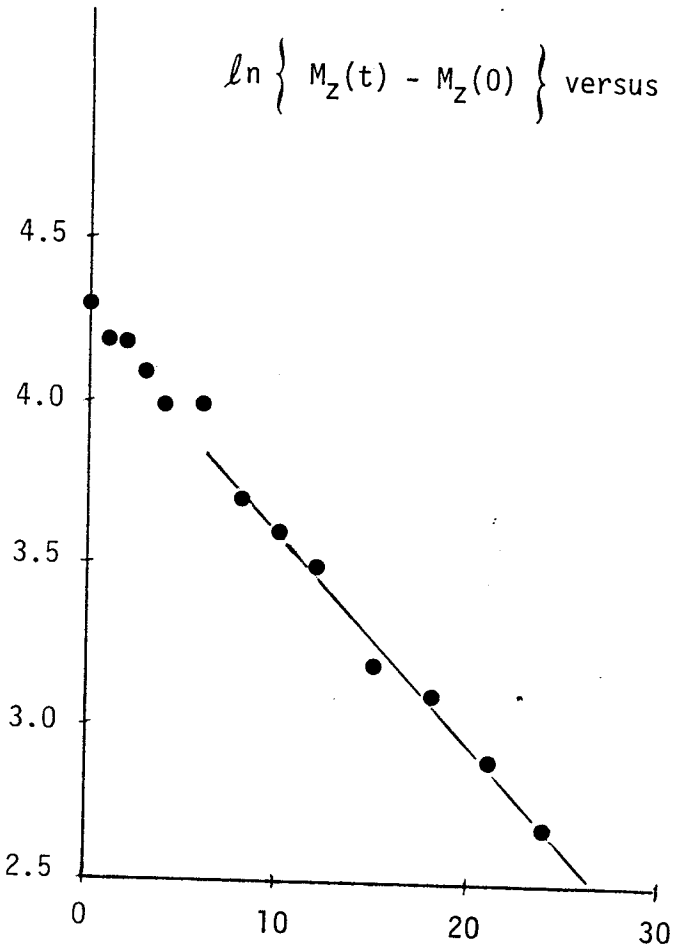

slope (after 6 sec.): $-0.0698\ sec^{-1}$

T_1: 14.25 sec.

Recovery Curve

Figure 24

Double resonance saturation transfer between protons A(I) and A(II) in HCOX at 278.1^{o}K as a function of time. The saturating field is applied to A(I) at t = 0 and is removed at t' = 0.

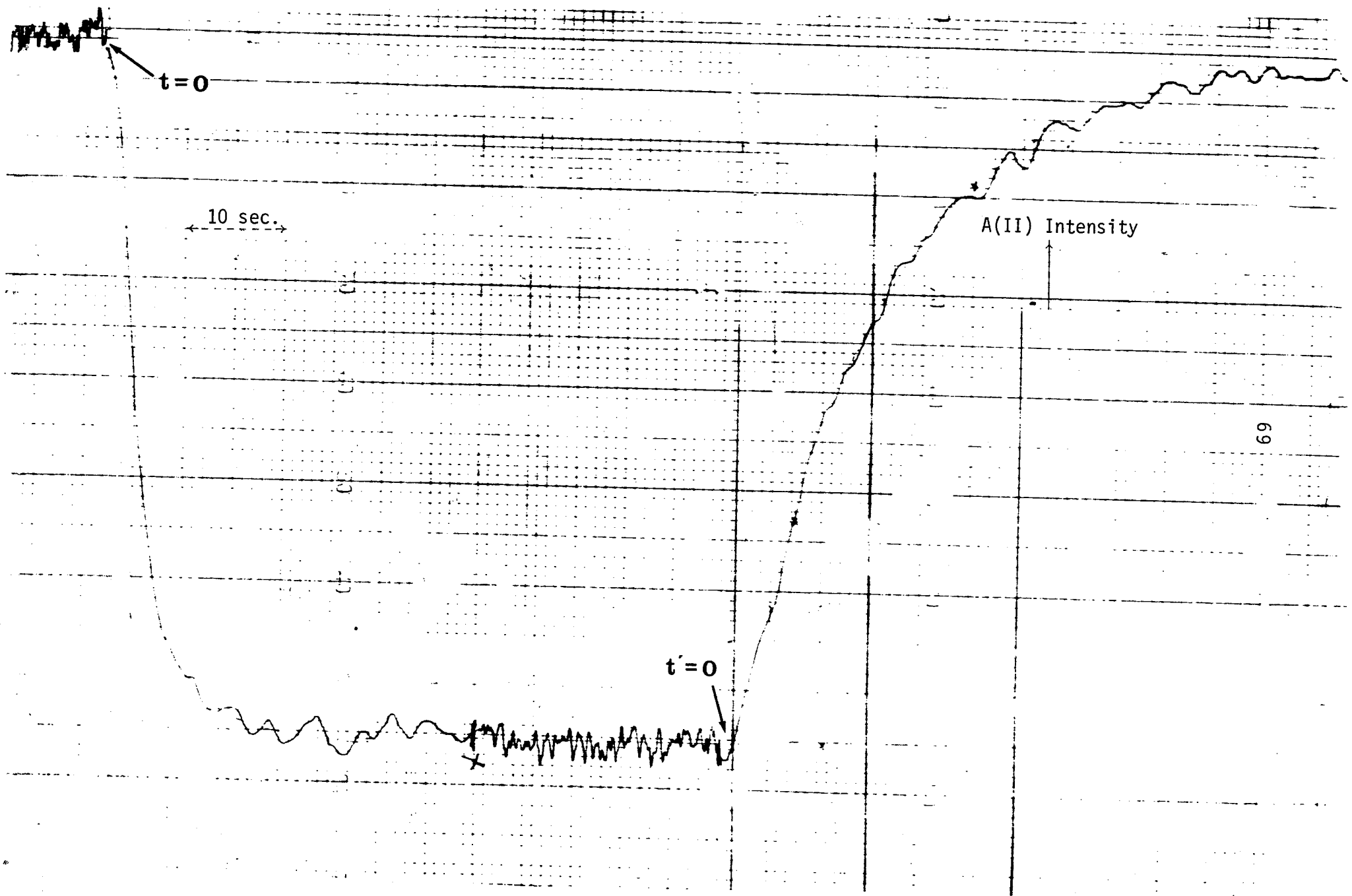
t = o
10 sec.
A(II) Intensity
t´= o

Figure 25

A plot of $\ln \left\{ M_z(t) - M_z(\infty) \right\}$ versus time and of $\ln \left\{ M_z(t) - M_z(0) \right\}$ versus time for the decay and recovery of proton A(II) at 278.1°K. Data obtained from Figure 24. $k = 0.264\ \text{sec}^{-1}$.

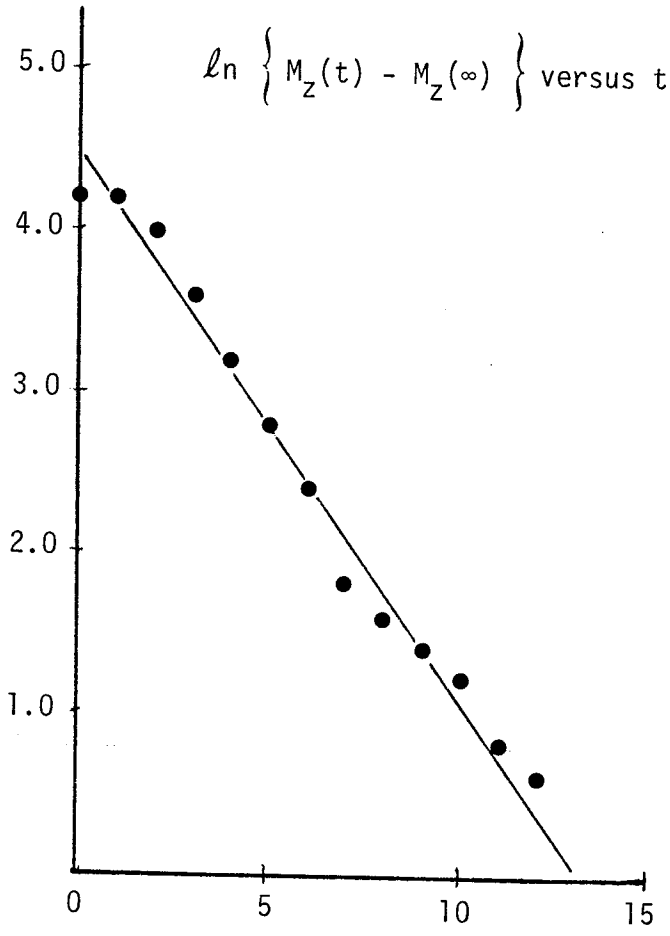

$\ell n \left\{ M_z(t) - M_z(\infty) \right\}$ versus time (sec.)

slope: $-0.3326\ sec^{-1}$

τ_1: 3.007 sec.

Decay Curve

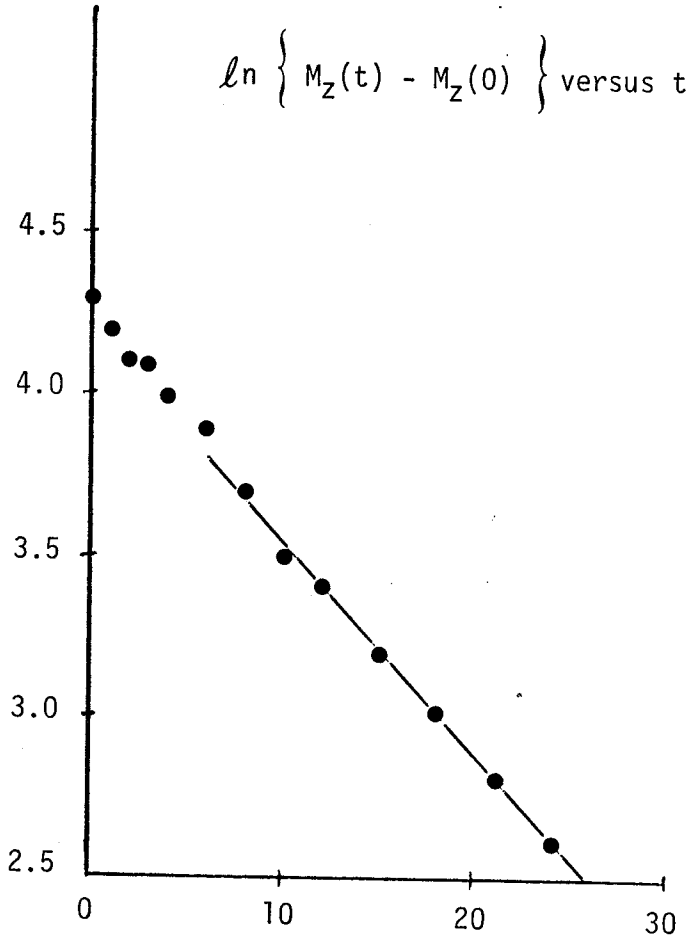

$\ell n \left\{ M_z(t) - M_z(0) \right\}$ versus time (sec.)

slope (after 6 sec.): $-0.0685\ sec^{-1}$

T_1: 14.55 sec.

Recovery Curve

Figure 26

Double resonance saturation transfer between protons A(II) and A(I) in HCOX at 278.1^{o}K as a function of time. The saturating field is applied to A(II) at t = 0 and is removed at t' = 0.

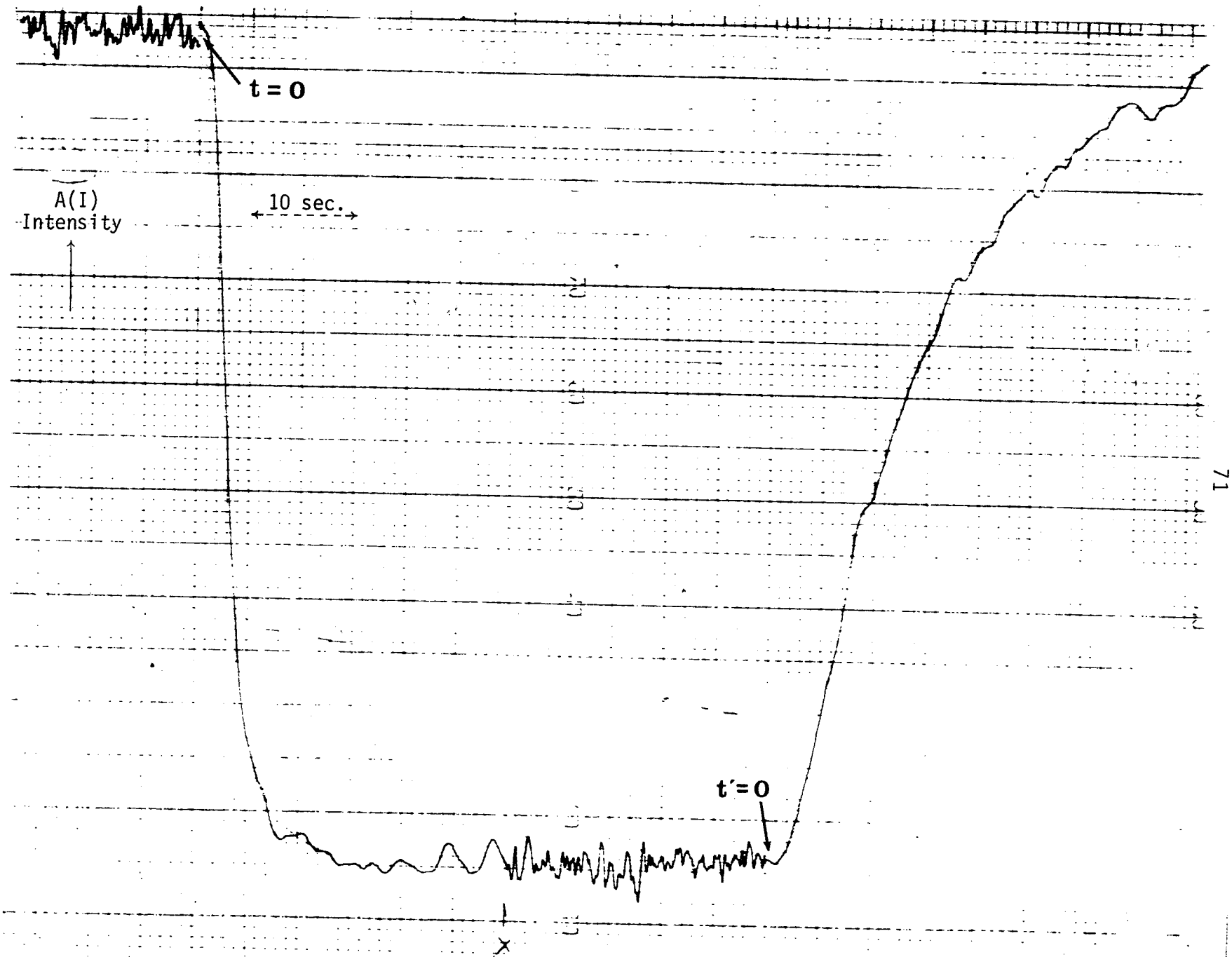
t = 0
A(I)
Intensity
10 sec.
t′ = 0

Figure 27

A plot of $\ln \left\{ M_z(t) - M_z(\infty) \right\}$ versus time and of $\ln \left\{ M_z(t) - M_z(0) \right\}$ versus time for the decay and recovery of proton A(I) at 278.1°K. Data obtained from Figure 26. $k = 0.283\ \text{sec}^{-1}$.

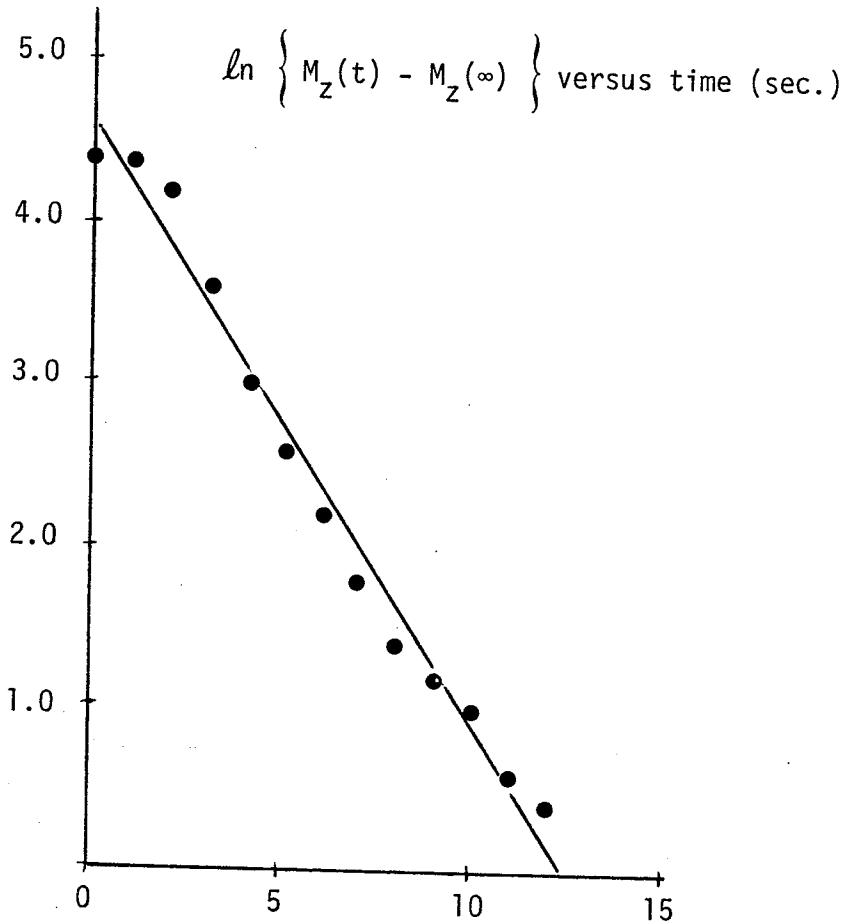

slope: $-0.3614\ \text{sec}^{-1}$

τ_1: 2.767 sec.

Decay Curve

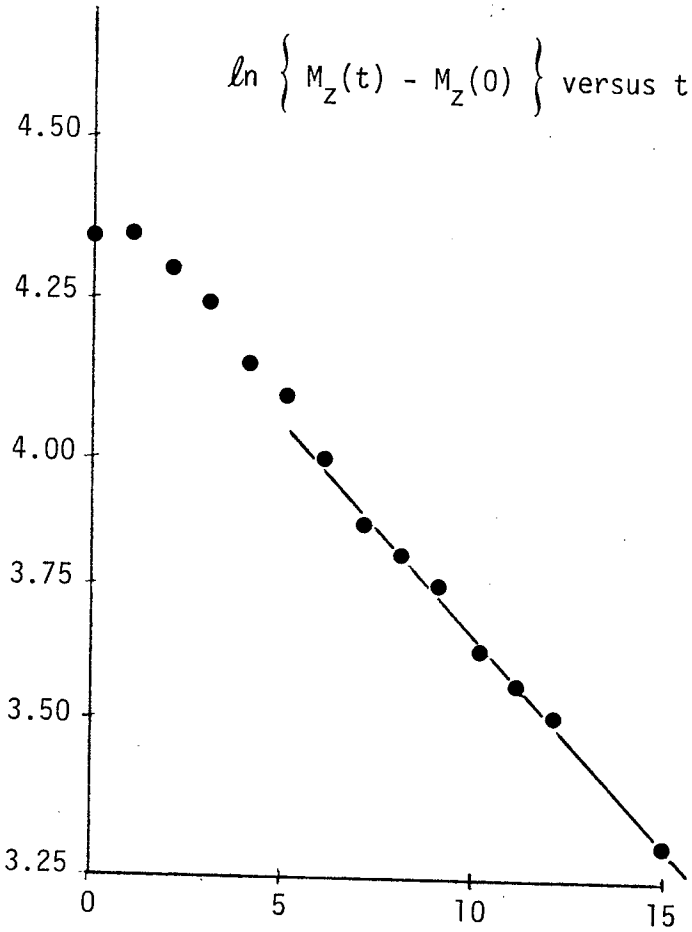

slope (after 6 sec.): $-0.0786\ \text{sec}^{-1}$

T_1: 12.65 sec.

Recovery Curve

Figure 28

Double resonance saturation transfer between protons A(I) and A(II) in HCOX at 268.1^{o}K as a function of time. The saturating field is applied to A(I) at t = 0 and is removed at t' = 0.

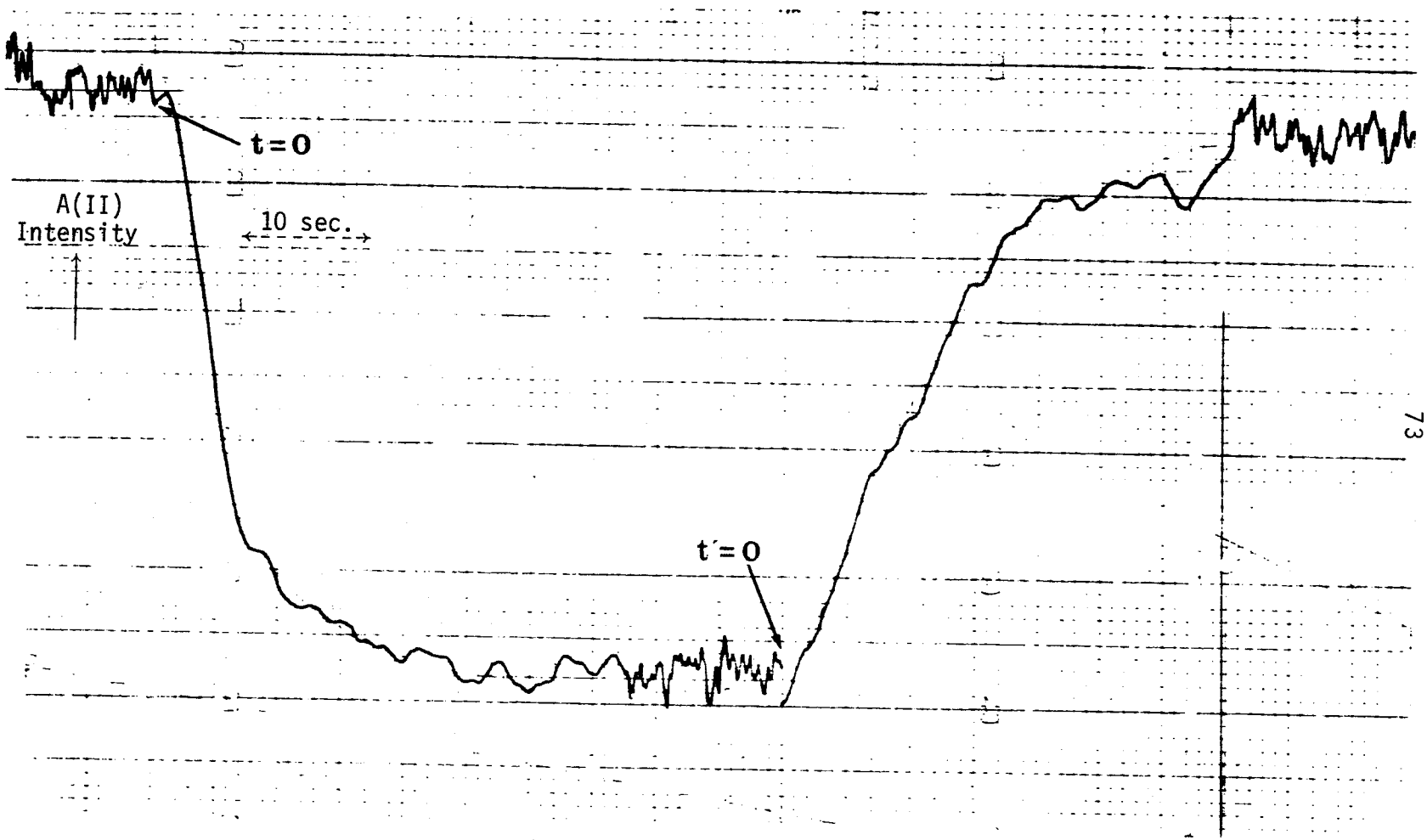
t=0
A(II)
Intensity
10 sec.
t´=0

Figure 29

A plot of $\ln \left\{ M_z(t) - M_z(\infty) \right\}$ versus time and of $\ln \left\{ M_z(t) - M_z(0) \right\}$ versus time for the decay and recovery of proton A(II) at 268.1°K. Data obtained from Figure 28. $k = 0.089\ \text{sec}^{-1}$.

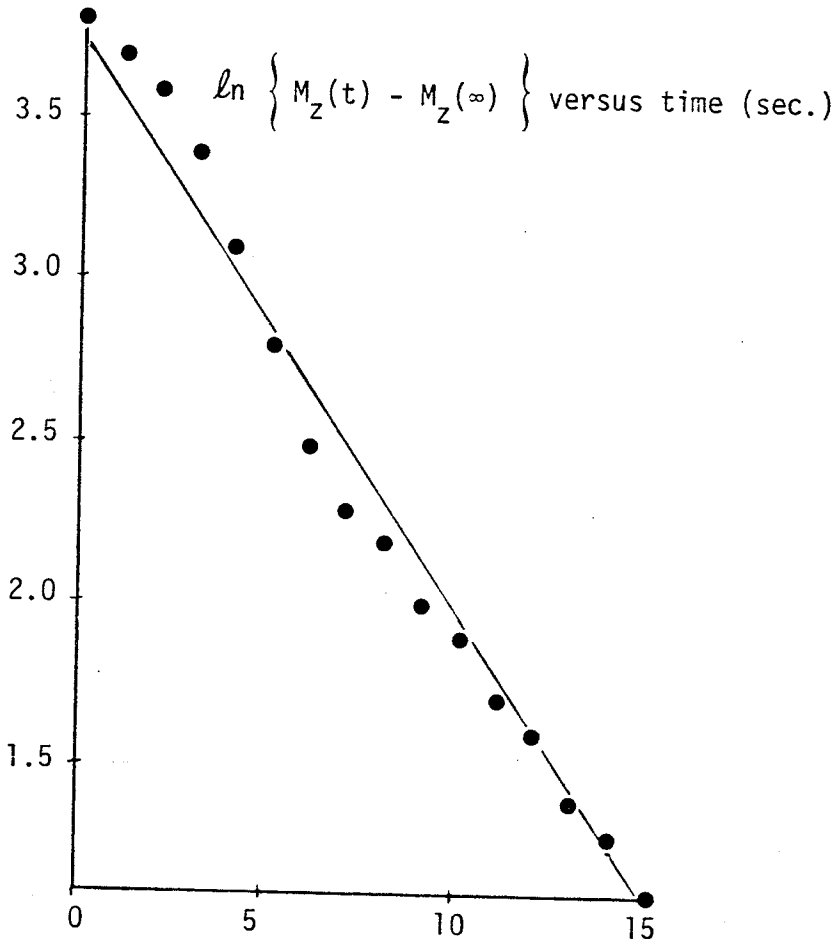

slope: $-0.1895\ sec^{-1}$

τ_1: 5.202 sec.

Decay Curve

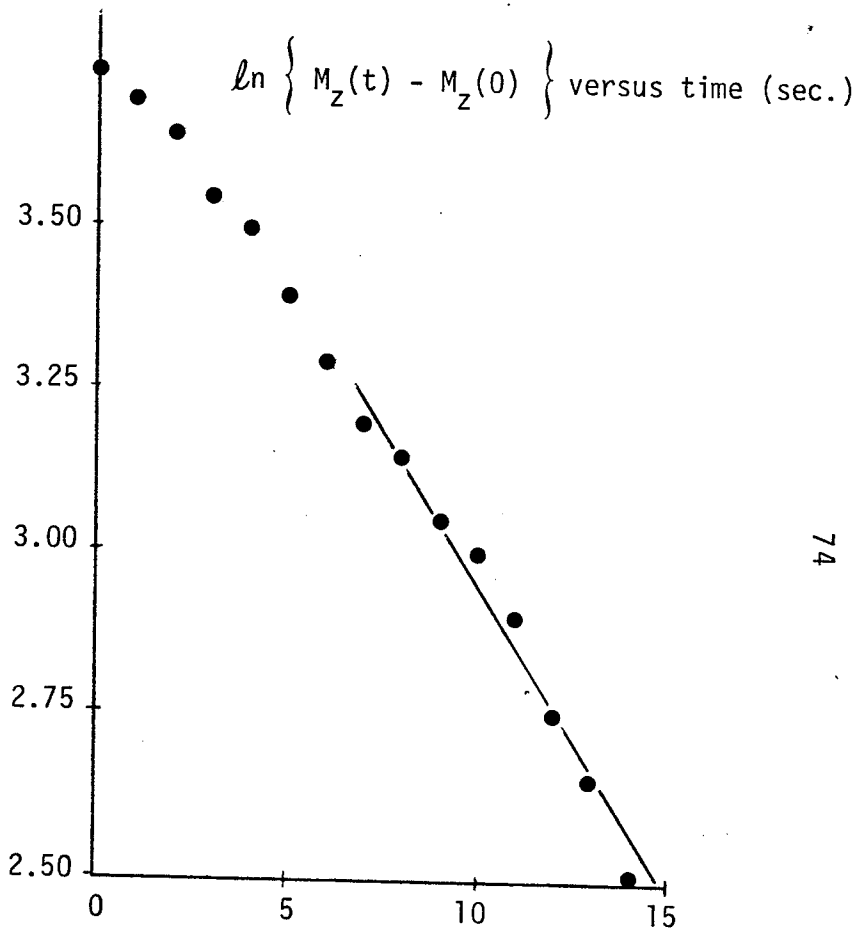

slope (after 6 sec.): $-0.1002\ sec^{-1}$

T_1: 9.845 sec.

Recovery Curve

Table 3

Data from double resonance saturation transfer experiment on HCOX in methylcyclohexane.

Temperature (^{o}K)	Proton Saturated*	Proton Observed*	Decay $M_z(\infty)/M_z(t)$	Decay τ_1 (sec.)	Recovery T_1 (sec.)**	Recovery k (sec^{-1})
268	A(I)	A(II)	.348	5.20	9.84	.089
268	A(I)	A(II)	.378	4.52	7.73	.093
					ave. k = .091 ± .02 sec^{-1}	
278	A(I)	A(II)	.203	3.01	14.6	.264
278	A(I)	A(II)	.196	2.86	13.4	.273
278	A(II)	A(I)	.102	2.77	12.6	.283
278	B(I)	B(II)	.200	2.81	14.2	.284
					ave. k = .276 ± .02 sec^{-1}	

* Labelled as in Figure 3.

** Estimated error ± 1.0 sec., resulting in a contribution of approximately 10% to k.

E. Calculation of Activation Parameters

The data necessary for both the Arrhenius plot and the Eyring plot are found in Table 4. The plot of ln k versus 1/T in Figure 30 is used to determine the energy of activation, Ea, and the frequency factor, A. The plot of ln (k/T) versus (1/T) in Figure 31 yields the enthalpy of activation, $\Delta H^{\neq}$, and the entropy of activation, $\Delta S^{\neq}$. The calculations assume that the transmission coefficient, κ, is unity (39).

In addition, Table 4 includes the calculated values of the free energy of activation using the equation

$$\Delta G^{\neq} = RT \ln \left[\frac{k_B T}{hk} \right] \qquad 4.1$$

at each temperature, T. The plot of $\Delta G^{\neq}$ versus T in Figure 32 is used to obtain $\Delta H^{\neq}$ and $\Delta S^{\neq}$ from equation 2.61 (40).

A summary of the activation parameters for HCOX and some related compounds studied by the same method is found in Table 5.

Table 4

Data employed for the determination of activation parameters Ea, log A, $\Delta H^{\neq}$ and $\Delta S^{\neq}$ for a 5 mole % solution of HCOX in methylcyclohexane.

Temperature* (^{o}K)	1/T (x 10^3)	k** (sec^{-1})	k/T (x 10^3)	ln k	ln k/T	$\Delta G^{\neq}$*** (kcal/mole)
268.0	3.73	.091 ± .02	3.39	-2.397	-7.987	16.90 ± .08
278.0	3.60	.276 ± .02	.993	-1.287	-6.908	16.95 ± .09
300.7	3.33	1.1 ± .2	3.66	0.095	-5.611	17.55 ± .18
305.8	3.27	2.6 ± .2	8.50	0.956	-4.767	17.33 ± .11
309.5	3.23	3.5 ± .2	11.31	1.253	-4.482	17.37 ± .10
314.1	3.18	4.2 ± .3	13.4	1.435	-4.315	17.52 ± .12
318.1	3.14	6.6 ± .3	20.7	1.887	-3.875	17.47 ± .10
320.0	3.12	8.0 ± .3	25.0	2.079	-3.689	17.45 ± .09
323.8	3.09	11.0 ± 0.4	34.0	2.398	-3.382	17.46 ± .09
327.1	3.06	12.5 ± .5	38.2	2.526	-3.264	17.56 ± .10
331.9	3.01	20.5 ± .5	61.8	3.020	-2.784	17.50 ± .09

Table 4 continued

336.4	2.97	26.0 ± 1	77.3	3.258	-2.560	17.59 ± .08
342.1	2.92	36.0 ± 1	105.2	3.584	-2.252	17.68 ± .08
347.5	2.88	49.0 ± 2	141.0	3.892	-1.959	17.76 ± .09
352.5	2.84	72 ± 2	204.3	4.277	-1.588	17.75 ± .08
356.2	2.81	104 ± 4	292.0	4.644	-1.231	17.68 ± .11
363.0	2.75	160 ± 5	440.8	5.075	-0.819	17.73 ± 0.10
369.0	2.71	198 ± 6	536.6	5.288	-0.622	17.87 ± 0.11

* All temperature with an error of ± 1^{o}, except at 369^{o}K where the error is ± 2^{o}K.

** Rate constants calculated using the shift data in Table 2 with T_2 from CH_2Cl_2 peak at each temperature; $J_{A(I)X(I)}$ = 0.45 Hz; all other J = 0.

*** Calculated from rate constant and temperature by equation 4.1.

Figure 30

Arrhenius plot of ln k versus 1/T. The data plotted are found in Table 4. $\ln k = (-7653 \pm 9)\frac{1}{T} + (26.01 \pm .03)$. Correlation coefficient: .9969

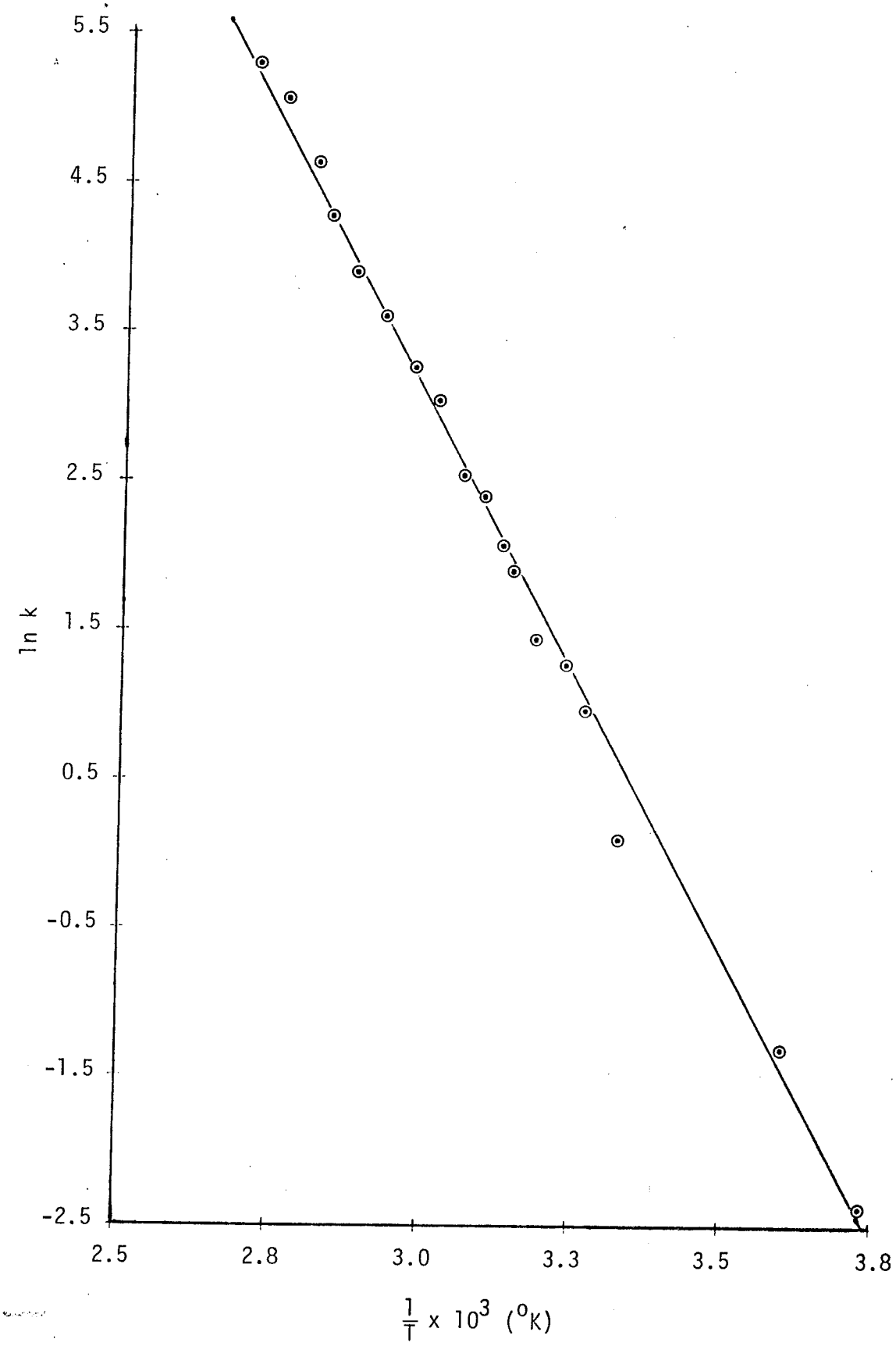
5.5
4.5
3.5
2.5
1.5
0.5
-0.5
-1.5
-2.5
ln k
2.5
2.8
3.0
3.3
3.5
3.8
$\frac{1}{T} \times 10^3$ (^oK)

Figure 31

Eyring plot of natural log k/T versus 1/T. The data plotted are found in Table 4.

$\ln k/T = (-7338 \pm 10)\frac{1}{T} + (19.25 \pm .025)$.

Correlation coefficient: 0.9967

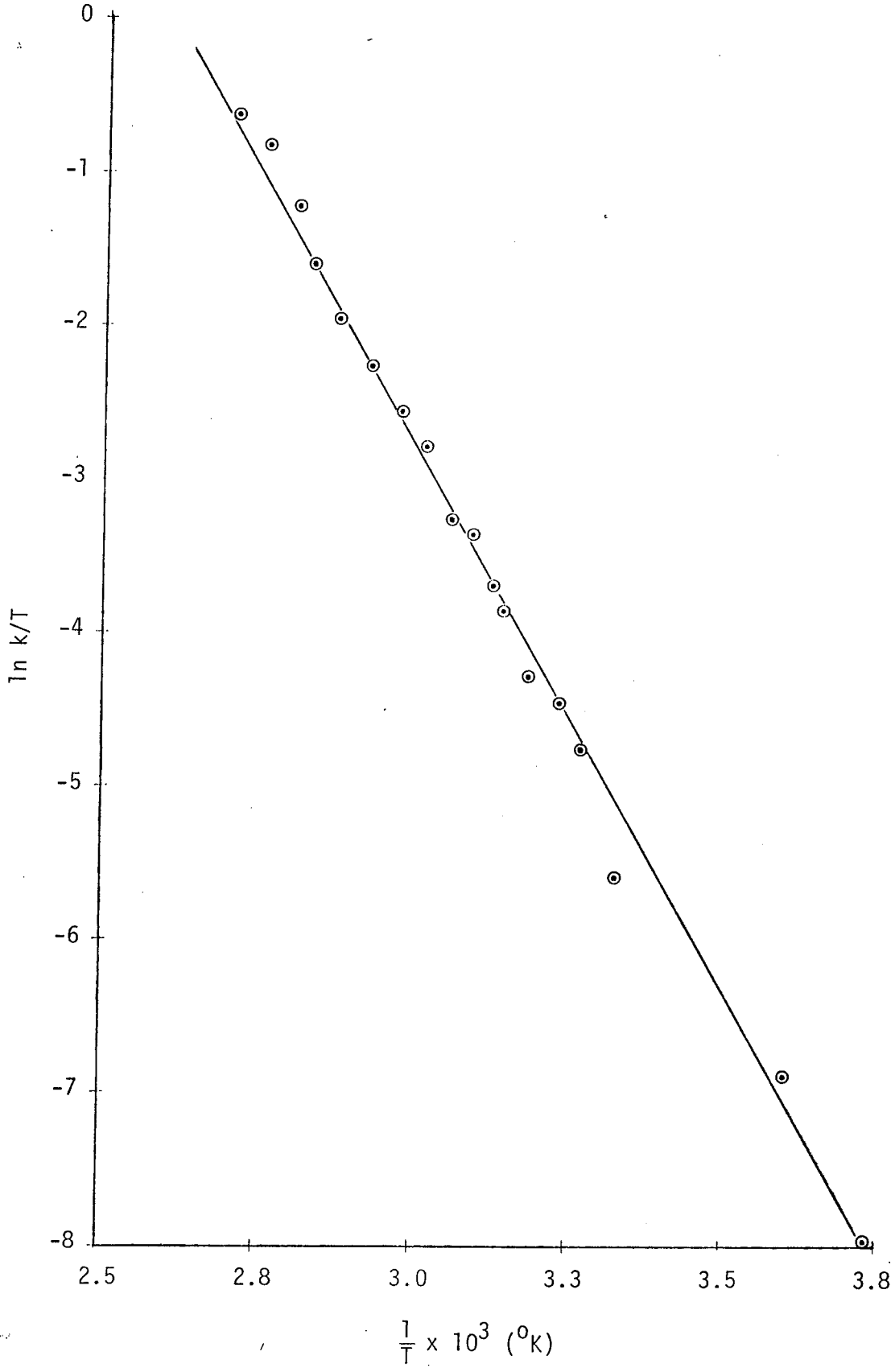
0
-1
-2
-3
-4
-5
-6
-7
-8
ln k/T
2.5
2.8
3.0
3.3
3.5
3.8
1/T x 10^3 (°K)

Figure 32

Plot of $\Delta G^{\neq}$ versus T. Data found in Table 4.

$\Delta G^{\neq} = 14.597 \pm 4.023 + (8.92 \pm 2.46)\ T$

Correlation coefficient: 0.956

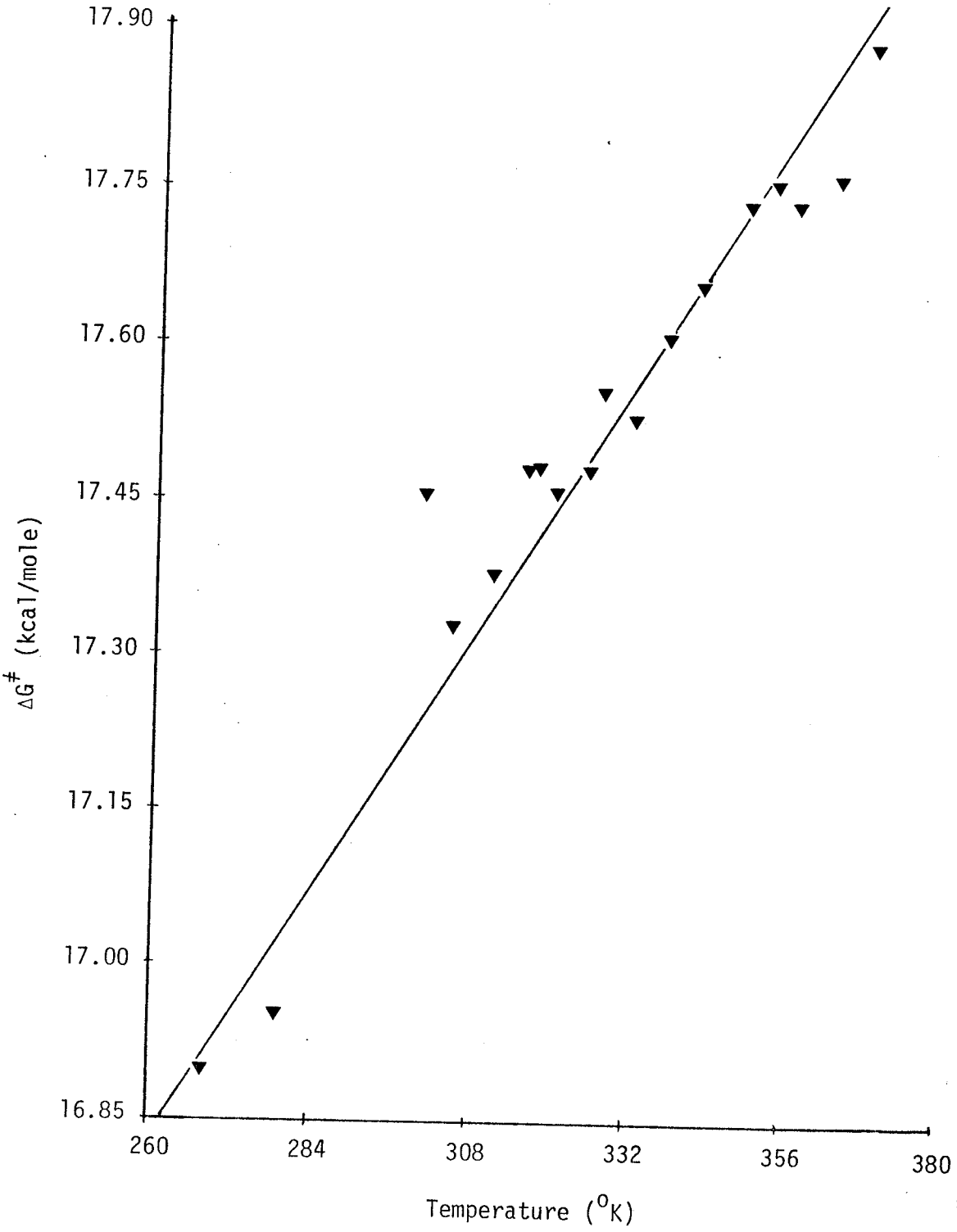
17.90
17.75
17.60
17.45
17.30
17.15
17.00
16.85
$\Delta G^{\neq}$ (kcal/mole)
260
284
308
332
356
380
Temperature (^{o}K)

Table 5

Summary of activation parameters for HCOX*, OCMX (32), OCPX (41), 2,3,6-PCT (42) and 2,4,6-PCT (43).

Compound	Solvent	Temp. (^{o}K)	Arrhenius Parameters		Transition State Parameters**		
			Ea (kcal/mole)	log A	$\Delta H^{\neq}$	$\Delta S^{\neq}$	$\Delta G^{\neq}$
HCOX	methylcyclohexane	298	15.3±0.3	11.3±.2	14.6±.3	-8.8±.8	17.2±.3
OCMX	toluene d_8	293	14.93±.13	12.45±.09	14.3±.14	-2.0±.5	14.9±.5
OCPX	toluene d_8	286	13.6±.4	11.3±.3	13.1±.4	-7.3±1.3	15.4±.1
2,3,6-PCT	toluene d_8	298	14.0±0.3	11.3±0.2	13.3±0.3	-7.0±0.7	15.4±0.1
2,4,6-PCT	toluene d_8	300	15.2±.2	12.7±.2	14.6±.2	-1.1±.7	14.9±.1
	methylcyclohexane		14.3±0.6	12.0±0.5	13.7±0.6	-4.4±2.2	15.0±0.2

* The values for the activation parameters of HCOX are obtained from the program ACTPAR (12) using the data from Table 4.

** kcal/mole for $\Delta H^{\neq}$, $\Delta G^{\neq}$ and cal/deg for $\Delta S^{\neq}$

F. Coalescence Temperature Calculations

It was not possible to determine the coalescence temperatures from the observed spectra. However, the rate constants at coalescence, k_c, for each of the three pairs of exchanging protons in HCOX were calculated using the expression (44)

$$k_c = \frac{\pi\Delta\nu}{\sqrt{2}} \qquad 4.2$$

where $\Delta\nu$ is the nonexchanging chemical shift difference of the proton resonance in the two conformers. These three rate constants were then substituted into the first-order equation obtained from the Arrhenius plot shown in Figure 30

$$\ln k_c = 26.01 - \frac{7653}{T_c} \qquad 4.3$$

to obtain the three coalescence temperatures, T_c. The value of the free energy of activation, $\Delta G^{\neq}$, at each of these coalescence temperatures was calculated using (45)

$$\Delta G^{\neq} = .004573\ T_c\ (9.97 + \log \frac{T_c}{\Delta\nu}) \qquad 4.4$$

and is shown with other data in Table 6.

Table 6

Summary of coalescence temperatures and $\Delta G^{\neq}$ values* for the protons of HCOX in methylcyclohexane.

Exchanging Proton	$\Delta\nu$ (Hz)	k_c (sec^{-1})	T_c (^oK)	$\Delta G^{\neq}$ (T_c) (kcal/mole)
H_A	47.1	104.6	358.3	17.8
H_B	39.2	87.1	355.3	17.8
H_X	9.6	21.3	333.5	17.6

* Calculated as described in this section.

G. Consideration of Error

1. Introduction

Experimental conditions under which data are obtained from the N.M.R. spectrometer must be carefully controlled to obtain usable information.

If line shape analysis is used to determine rate constants there should exist no saturation, excessive filtering or magnetic field inhomogeneity. The sample should spin smoothly in a well-regulated thermal environment. Consistent effort was made to ensure that optimum conditions prevailed for each spectrum. Maximum scanning speed was 0.05 Hz/sec and the filter was set at 14; no evidence of saturation was found at any time. Any distortions which may have gone undetected are least significant about the coalescence point, increasing as the temperature changes. Thus the data obtained by this method is most reliable near coalescence, and the reliability increases for any system like HCOX that has a series of temperatures at which coalescence occurs.

The error in determining the effective spin-spin relaxation time, T_2', value has been shown to be critical for the determination of $\Delta H^{\neq}$ and $\Delta S^{\neq}$ values (41). Although a linear Arrhenius plot may be obtained, the values of $\Delta H^{\neq}$ may be inaccurate and those for $\Delta S^{\neq}$ may often be physically unreasonable (46) due partly to the limited temperature range involved and partly to the problem of obtaining accurate exchange rates. The errors introduced by estimating the values of shift

differences and linewidths in the absence of exchange are larger than the Arrhenius plot might indicate (47,48). In the present case, the use of data from the double resonance saturation transfer method significantly reduces such errors.

If the double resonance saturation transfer method is used, optimization of experimental conditions involves the consideration of some additional parameters. Incomplete saturation of the irradiated site and inaccurate adjustment of the frequencies of the audio generator and/or of the recorder can significantly alter the response from the irradiated system and must be avoided.

2. Errors in determining the exchange rate constant, k

a) Line shape analysis

The rotation of the two dichloromethyl groups in HCOX has been treated as an uncoupled, equally-populated, two-site system undergoing synchronized exchange. For such a system the computer program DNMR2 (38) will generate line shapes if the chemical shifts of the proton at each site, the relative populations of the two conformers, the linewidth of an absorption signal in the absence of exchange, the exchange rate constant and various scaling parameters are input. Since the calculated line shape was used to determine k, the error in the rate constant is related to the error of the first three parameters above. These will now be discussed individually.

i) Errors in chemical shifts

The determination of chemical shifts in the absence of exchange for all protons in the two conformers is a necessary prerequisite to obtaining accurate rate constants. The advantage of having coalescence temperatures above ambient lies in the wider range over which chemical shifts can be measured. The resulting extrapolation of the chemical shift from the slow exchange region to the faster exchange at higher temperatures is more accurate than assuming that the chemical shifts are invariant with temperature (46). For HCOX the measured maximum change in chemical shift for any proton was 2.5 Hz in the temperature range, $-20^{o}C$ to $98^{o}C$. As shown in Figures 4 and 5, the differences between the resonances of any one proton in the two conformers changed less than 1.0 Hz in the same temperature range. Any error arising from an inaccurate estimate of chemical shifts would be greatest in the extrapolated high temperature region. Since methylcyclohexane boils at $100.9^{o}C$ (34), this temperature region was not investigated, reducing any error contribution due to this effect.

ii) Errors in relative population determination

The difference in calculated spectra when $k > 40\ sec^{-1}$ between assigned relative populations of 0.96:1.00 and those with relative populations of 1.04:1.00 was not detectable. When the exchange rate constant was less than $40\ sec^{-1}$ there was a slight difference in relative peak height but none in peak position. The error in the assignment of equal populations to each of the two conformers for HCOX is not considered a contributing factor to the error in the exchange rate constant.

iii) Errors in linewidth in absence of exchange

Some investigators have used a constant-input linewidth (49) determined below the slow exchange limit. Others have observed that the principal cause of line-broadening is due to magnetic field inhomogeneity (50-52) and have used the width of the tetramethylsilane (TMS) signal as observed at each temperature. Neither observation may be universally applicable.

In general, the half height linewidth, $W_{1/2}$, of an absorption peak in the absence of exchange may be written as a sum of terms (47)

$$W_{1/2} = \frac{1}{\pi T_2} \simeq \frac{1}{\pi T_2}\,\mathrm{inh} + \frac{1}{\pi T_2}\,\mathrm{sc} + \frac{1}{\pi T_2}\,\mathrm{dd} + \frac{1}{\pi T_2}\,\mathrm{LR} \qquad 4.5$$

which includes the contributions from the magnetic field inhomogeneity, scalar coupling, dipole-dipole interactions, and any unresolved long-range proton-proton couplings, respectively. The last term is considered negligible for HCOX, and the first two terms should be similar for HCOX and CH_2Cl_2 which is used as the reference. Any error in linewidth must then result from the effect of intramolecular and intermolecular dipole-dipole interactions. For small molecules such interactions are much less significant than the magnetic field inhomogeneity and for molecules with molecular weight $\geq$ 500 amu the effect may be an increase of as much as 1 Hz to the linewidth at $-30^{o}C$ (47).

The molecular weight of HCOX is 347.3 amu and dipole-dipole interactions should be considered. The viscosity of the methylcyclo-

hexane solution was low (ca. 0.735 centipoise at 20°C) (34) and the contribution to the spin-spin relaxation rate $1/T_2^{dd}$ equals the spin-lattice relaxation rate, $1/T_1$ (47). Thus the largest contribution for the temperature range studied by this method would be 0.07 Hz at 20°C. Any error introduced by omitting this contribution becomes insignificant when the exchange process dominates the width of the line shape. Thus the use of the experimental linewidth of methylene chloride is justified at temperatures above 30°C where the maximum error would be 2% if other parameters remained constant. At lower temperatures the increasing viscosity and the reduction in the rate of exchange would cause a significant error. This effect may account for the deviation of values in the free energy of activation plot (Figure 32) below 30°C.

b) Double resonance technique

Using this method, the rate constant is determined by finding the difference between the two terms $1/\tau_1$ and $1/T_1$ (equation 2.42). The error in k will be equal to the larger of the errors of these two terms. Since τ_1 and T_1 are calculated from the decay and the recovery of the signal any factor influencing the signal intensity will affect the rate constant obtained. Conditions were checked prior to each determination to eliminate or minimize the errors due to experimental conditions. Complete saturation was assured by increasing the power of the irradiating field until the exchange-site-signal did not decay further upon increasing the power. This value was then used for all subsequent

measurements. Data analysis was hampered by noise factors and, since the decay period was short, this may well be the dominant error source. The $1/\tau_1$ term is found from the slope of the $\ln \left[M_z(t) - M_z(\infty)\right]$ versus time plot and its error may well be from three to five times that indicated by a least squares fit. The second term, $1/T_1$, can be determined in two ways, from the slope of the recovery data and from the magnetization ratios (equation 2.49). When using the plot of $\ln (M_z(t) - M_z)$ versus time the contribution of the first terms must be allowed to decay before the slope can be used to determine the spin-relaxation time. The complete equation is

$$\ln (M_z^B(t) - M_z^B) = \ln \left[c_1 \exp (-\lambda_1 t) + c_2 \exp (-\lambda_2 t)\right] \qquad 4.6$$

if $T_{1B} \sim \tau_B$ then $\lambda_1 \sim 3\lambda_2$ and $c_2 \sim 3c_1$ from equation 2.51 to 2.54. Thus $\left[\frac{c_1}{e^{\lambda_1 t}}\right]$ will originally be smaller and will decrease much more quickly with time than the second term on the right of equation 4.6.

In each case the first six values from an arbitrary zero were omitted in determining the slope. The value of T_{1B} obtained by this method was checked against that obtained by using equation 2.49. The trial was discarded if the difference between the two determinations exceeded five per cent of the first value. The difference between the two terms, $1/\tau_{1B}$ and $1/T_{1B}$, results in an error of at least five per cent for the value of k and may be even higher. In absolute terms the result

is still quite good as indicated in Table 3.

3. Errors in temperature - measurement and drift

The conversion of millivolt readings from the iron-constantan thermocouple to a temperature reading is assumed to be free of error. If equilibrium conditions can be assumed for all determinations, the values obtained should be quite reliable. However, the temperature reading taken before and that taken after a spectrum was obtained were usually different. The drift in temperature varied between 0.04 and $0.70^{o}K$. Repeated trials under constant conditions indicated that random errors were about $0.03^{o}K$ on ten trials. Reporting the temperature to within $1^{o}K$ should provide a tolerance greater than that required by consideration of these factors.

4. Errors in the calculation of activation parameters

Two different methods were employed to determine the exchange rate constants and they appear to be complementary. Systematic error should therefore be less suspect than if only a single method were used.

a) Thermodynamic functions

The statistical treatment of data produces the results shown in Table 7. The results obtained from the different treatments display excellent agreement within the statistical deviation. Since the free energy of activation, $\Delta G^{\neq}$, is related to $\Delta H^{\neq}$ and $\Delta S^{\neq}$ by equation 2.61 and will obviously also show consistent values, it has not been

included. Thus the statistical treatment to obtain "average" values does not cause significant changes in the errors of even these most sensitive parameters.

The standard errors reported in Table 5 for HCOX were obtained from Binsch's program, ACTPAR (12), which incorporates errors in k and in T to determine the errors in the activation parameters.

A recalculation using a value of one-half* for the transmission coefficient, $\kappa(39)$, lowered the value of $\Delta S^{\ddagger}$ by 1.4 e.u. and the value of $\Delta G^{\ddagger}$ by 0.42 kcal/mole at $298^{o}K$; $\Delta H^{\ddagger}$, of course, remains unaffected.

b) Energy of activation

The standard deviation of the activation energy obtained from a least squares analysis of the Arrhenius plot is much too small because the errors in the input parameters are ignored in the calculation. These can be explicitly incorporated by using the equation (53)

$$\left[\frac{\sigma_{Ea}}{Ea}\right]^2 \simeq \frac{2T^2}{\Delta T^2}\left[\frac{\sigma_T}{T}\right]^2 + 2\left[\frac{1}{\Delta(\ln k)}\right]^2\left[\frac{\sigma_k}{k}\right]^2 \qquad 4.7$$

where σ_T is the standard deviation of the temperature, σ_k is the standard deviation of the exchange rate constant, ΔT is the temperature range under study and $\Delta(\ln k)$ is the range of the ln k values. If T and k are the temperature and exchange rate at coalescence respectively, σ_T is assumed to be $1^{o}K$, σ_k is 4 when k is 104 and T is 356.8, ΔT is

---

* Not likely to be the case as $\kappa = \frac{1}{2}$ assumes that the probability of the transition state reverting to the starting point is as great as the probability that it will proceed to "product".

Table 7

Statistical check on thermodynamic parameters for the hindered rotation of the side chain groups of HCOX in methylcyclohexane at $298^{o}K$.

Thermodynamic Function	Method of Calculation	Source	Value Obtained
$\Delta H^{\neq}$	1. $\Delta H^{\neq} = Ea - RT$	Ea from slope of Arrhenius plot Figure 30	14.62±.02 kcal/mole
	2. $\Delta H^{\neq}$ = -R x slope of Eyring plot	Figure 31	14.58±.02 kcal/mole
	3. $\Delta H^{\neq}$ = intercept of $\Delta G^{\neq}$ vs. T plot	Figure 32	14.60±4.0 kcal/mole
$\Delta S^{\neq}$	1. $\Delta S^{\neq} = \frac{\Delta H^{\neq} - \Delta G^{\neq}}{T}$; $\Delta H^{\neq}$ via Arrhenius plot $\Delta G^{\neq}$ from equation 4.1	Figure 30	-9.8±0.6 e.u.
	2. $\Delta S^{\neq}$ = (intercept - 23.06*) x R	from Figure 31	-8.8±0.6 e.u.
	3. $\Delta S^{\neq}$ = -slope	from Figure 32	-8.9±2.4 e.u.

* if $\kappa = 1.00$

101^{o} and $\Delta(\ln k)$ is 7.663, then the standard error in activation energy is approximately 0.24 kcal/mole or about ten times the error obtained from the Arrhenius plot. The computer program, ACTPAR (12), indicates an error of 0.3 kcal/mole.

To obtain a range indicative of maximum error for the activation energy the minimum and maximum values of k and T were obtained from Table 4 and combined with the value of ln A from Figure 30. These were substituted into (54)

$$\ln k = \ln A - \frac{Ea}{RT} \qquad 4.8$$

in order to obtain a maximum and minimum value of Ea. Using the data of Table 4 the calculated maximum error in the activation energy is ±0.45 kcal/mole or an error of approximately three per cent.

In the preceding discussion both $\Delta H^{\neq}$ and Ea have been assumed to be invariant with temperature. Otherwise the values for the rate constants would be affected and the plots of Figures 30 and 31 would yield smooth curves. However, these two are related by the equation (52)

$$\Delta H^{\neq} = Ea - RT \qquad 4.9$$

which shows that only one can be constant. The error introduced for a $100^{o}K$ temperature range is 0.2 kcal which is an uncertainty less than that reported for either parameter.

H. Comparison of Activation Parameters with Related Compounds

The free energy of activation may be the most reliable measure of differences in hindered rotation because it is the least sensitive to error (46-49). Table 5 uses these values as the basis for comparing the barrier to hindered rotation in some selected compounds.

Earlier studies rationalized the increase in $\Delta G^{\neq}$ from α,α,2,4,6-pentachlorotoluene (2,4,6-PCT), $\Delta G^{\neq}$ = 14.9 ± 0.1 kcal/mole in toluene d_8 (43), to α,α,2,3,6-pentachlorotoluene (2,3,6-PCT), $\Delta G^{\neq}$ = 15.4 ± 0.1 kcal/mole in toluene d_8 (29), on the basis of the buttressing effect of adjacent chlorine atoms on the ring (42). The barrier for α,α,α',α', 2,3,5,6-octachloro-para-xylene (OCPX), $\Delta G^{\neq}$ = 15.4 ± 0.1 kcal/mole in toluene d_8 (41) appeared to confirm this explanation. However, such rationale does not account for the free energy of activation being lower for α,α,α',α',2,4,5,6-octachloro-meta-xylene (OCMX), $\Delta G^{\neq}$ = 14.9 ± 0.5 kcal/mole in toluene d_8 (32), and an explanation has been advanced suggesting that buttressing may increase the ground state energy more than the transition state energy (41). In addition the effects of electron withdrawing substituents on the aromatic ring may produce distortions which are presently not predictable. If each of the dichloromethyl groups of α,α,α',α',α",α",2,4,6-nonachloromesitylene (NCM) were treated as an independent rigid rotor flanked by a single chlorine on each side, the free energy of activation should be comparable to that for 2,4,6-PCT; whereas the consideration of an "effective" size (55) for the dichloromethyl groups suggests that the $\Delta G^{\neq}$ value be comparable to OCMX. The experimental value, $\Delta G^{\neq}$ = 16.1 ± 0.06 kcal/mole

in toluene d_8 (32), indicates that these trends are not reliably predicted using buttressing effects. Since the author is not aware of any method of determining ground state energies, the de facto results lend themselves to speculation at present.

Two molecules that are very similar to HCOX have been studied (37), α,α,α',α',3,4,5,6-octachloro-ortho-xylene (OCOX) and α,α,α',α',3,6-hexachloro-ortho-xylene (HXCOX). The free energy of activation of these two molecules should correspond closely to that of HCOX as all three should exhibit similar "cog-wheel" effects and the ring-distortion and/or buttressing due to the chlorine atoms on the ring would predict that the $\Delta G^{\neq}$ value for HCOX lies between HXCOX and OCOX. With $\Delta G^{\neq}$ for OCOX at coalescence equal to 17.7 kcal/mole and $\Delta G^{\neq}$ for HXCOX at coalescence equal to 17.4 kcal/mole (37), this would indicate that the coalescence value for HCOX in tetradecane should fall in the range 17.4 to 17.7 kcal/mole. A direct comparison is not possible because HCOX was studied in methylcyclohexane with $\Delta G^{\neq}$ at coalescence of 17.7 kcal/mole (Figure 33). If an error of 0.3 kcal/mole can be assumed for each of these three results, then the expected relationship is not contradicted.

Figure 33

$\Delta G^{\ddagger}$ values for HCOX and some related compounds.

All values in kcal/mole with solvent and temperature in parentheses.

Abbreviations used:		
	Toluene d_8	Td_8
	methylcyclohexane	MC
	tetradecane	TDC
	methylene chloride	MCl

Data from references as listed in text.

2,4,6-PCT

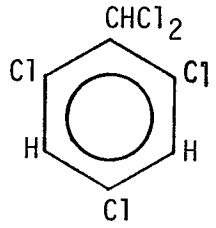

$\Delta G^{\neq}$= 14.9 (Td_8)
= 15.0 (MC)
(304°K)

2,3,6-PCT

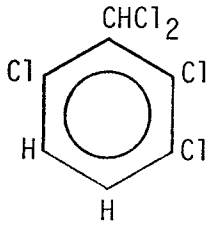

$\Delta G^{\neq}$= 15.4 (Td_8)
(298°K)

OCPX

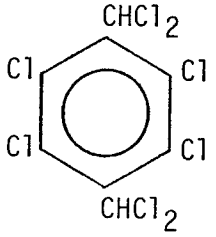

$\Delta G^{\neq}$= 15.4 (Td_8)
(286°K)

OCMX

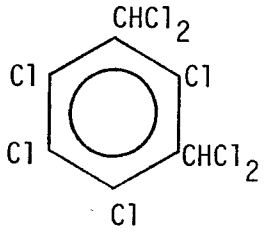

$\Delta G^{\neq}$= 14.9 (Td_8)
(293°K)

NCM

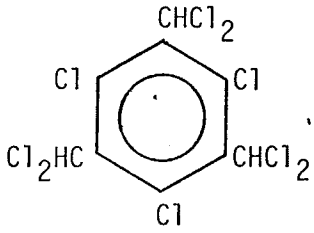

$\Delta G^{\neq}$= 16.5 (MCl)
= 16.1 (Td_8)
(304.6°K)

HXCOX

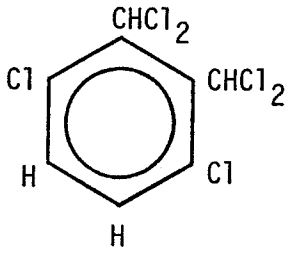

$\Delta G^{\neq}$= 17.4 (TDC)
(350°K)

HCOX

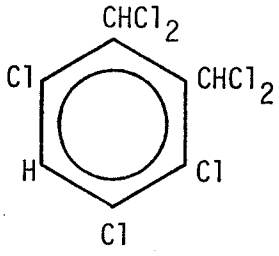

$\Delta G^{\neq}$= 17.2 (298°K)
= 17.8 (358°K)
(MC)

OCOX

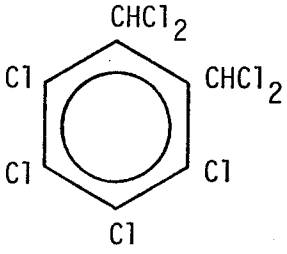

$\Delta G^{\neq}$= 17.7 (TDC)
(356°K)

V. SUMMARY AND CONCLUSIONS

A study of the hindered rotation of the dichloromethyl groups of α,α,α',α',3,4,6-heptachloro-ortho-xylene (HCOX) has been conducted using a complete line shape analysis supplemented with the double resonance saturation transfer technique. The study was carried out on a 5 mole % solution of HCOX in methylcyclohexane over a temperature range of 268 to 369^{o}K. The spectrum was assigned to the corresponding protons in each of the two conformers by the double resonance method and by steric crowding considerations. A study of relative populations was made at lower temperatures only.

Activation parameters were calculated using the Arrhenius equation and transition state theory and are recorded in Table 4. Comparison of the results of the compounds in the table favor the suggestion that synchronization of the two dichloromethyl groups in the ortho position increase the energy barrier to rotation. The results compare favourably with HXCOX and OCOX obtained in a different solvent. The "cog-wheel" effect producing a very ordered transition state rationalizes the negative value of the $\Delta S^{\ddagger}$ term.

It is concluded that there are two contributions to the barrier to rotation in HCOX. The steric hindrance between the chlorine atoms on the ring and the chlorine atoms on the methyl carbon produces an effect comparable to that in 2,3,6-PCT, 2,4,6-PCT and OCPX and OCMX. Added to this is the restriction to rotation due to the proximity of the two dichloromethyl groups.

BIBLIOGRAPHY

1. J.A. Landgrebe. Theory and Practice in the Organic Laboratory. D.C. Heath and Co., Toronto, 1973, Chapter 9.

2. J. English, Jr. and H.G. Cassidy. Principles of Organic Chemistry. McGraw-Hill Book Co., Toronto, 1961, Chapter 2.

3. A.A. Allinger, M.P. Cava, P.C. De Jongh, C.R. Johnson, N.A. Lebel, and C.L. Stevens. Organic Chemistry, 2nd edition. Worth Publishers, New York, 1976, Chapter 3.

4. F.A.L. Anet and R. Anet. in Determination of Organic Structures by Physical Methods, Vol. 3. F.C. Nachod and J.J. Zuckerman (Editors). Academic Press, New York, 1971.

5. C.S. Johnson, Jr. Advan. Mag. Res. 1, 33 (1965).

6. J.A. Pople, W.G. Schneider, and H.J. Bernstein. High Resolution Nuclear Magnetic Resonance. McGraw-Hill Book Co., New York, 1961, Chapter 10.

7. A. Abragam. The Principles of Nuclear Magnetism. Oxford Press, New York, 1961.

8. S. Forsen and R.A. Hoffman. J. Chem. Phys. 39, 2892 (1963).

9. F.A.L. Anet and A.J.R. Bourn. J. Am. Chem. Soc. 89, 760 (1967).

10. G. Binsch. J. Am. Chem. Soc. 91, 1304 (1969).

11. H. Gyulai. M.Sc. thesis, University of Manitoba, 1970.

12. G. Binsch. J. Am. Chem. Soc. 94, 2770 (1972).

13. C.P. Schlichter. Principles of Magnetic Resonance. Harper and Row, New York, 1963, Chapter 2.

14. H.S. Gutowsky, D.W. McCall, and C.P. Schlichter. J. Chem. Phys. 21, 279 (1953).

15. H.S. Gutowsky and A. Saika. J. Chem. Phys. 21, 1688 (1953).

16. H.S. Gutowsky and C.H. Holm. J. Chem. Phys. 25, 1228 (1956).

17. H.M. McConnell. J. Chem. Phys. 28, 430 (1958).

18. H. Carrington and A.D. McLachlan. Introduction to Magnetic Resonance. Harper and Row, New York, 1967, Chapter 2.

19. J.W. Emsley, J. Feeney, and L.H. Sutcliffe. Progress in NMR Spectroscopy, Vol. 2. Pergamon Press, Toronto, 1967, Chapter 4.

20. J. Kaplan. J. Chem. Phys. 28, 278 (1958).

21. S. Alexander. J. Chem. Phys. 37, 967 (1967).

22. G.M. Whitesides. Ph.D. thesis, California Institute of Technology, 1964.

23. S. Forsen and R.A. Hoffman. Acta. Chem. Scand. 17, 1787 (1963).

24. S. Forsen and R.A. Hoffman. J. Chem. Phys. 40, 1189 (1964).

25. G.M. Barrow. Physical Chemistry. McGraw-Hill Book Co., Toronto, 1966, Chapter 15.

26. F. Daniels, R.A. Alberty, J.W. Williams, C.D. Cornwell, P. Bender, and J.A. Harriman. Experimental Physical Chemistry, 7th edition. McGraw-Hill Book Co., New York, 1956.

27. B.J. Fuhr, B.W. Goodwin, H.M. Hutton, and T. Schaefer. Can. J. Chem. 48, 1558 (1970).

28. J. Peeling, T. Schaefer, and C.M. Wong. Can. J. Chem. 48, 2839 (1970).

29. M.A.H. Stewart, T. Schaefer, H.M. Hutton, and C.M. Wong. Can. J. Chem. 49, 1085 (1971).

30. J. Peeling, B.W. Goodwin, T. Schaefer, and C.M. Wong. Can. J. Chem. 49, 1489 (1971).

31. B.H. Barber and T. Schaefer. Can. J. Chem. 49, 789 (1971).

32. J. Peeling, B.W. Goodwin, T. Schaefer, and J.B. Rowbotham. Can. J. Chem. 51, 2110 (1973).

33. C. Roussel, M. Chenon, and J. Metzger. J. Tetra. Lett., 1861 (1971).

34. J.A. Riddick and W.B. Bunger. Techniques of Chemistry, Vol. II, 3rd edition. Wiley-Interscience, Toronto, 1970, page 85.

35. M. Barfield and B. Chakrabarti. Chem. Rev. 69, 757 (1969).

36. J. Peeling, L. Ernst, and T. Schaefer. Can. J. Chem. 52, 849 (1974).

37. V. Mark and V.A. Pattison. Chem. Comm., 553 (1971).

38. G. Binsch and D.A. Kleier. The Computation of Complex Exchange-broadened NMR Spectra. Program 140, Quantum Chemical Program Exchange, Indiana University, 1969.

39. W.F. Shuhan. J. Chem. Ed. 47, 254 (1970).
D. Houalla, R. Wolf, D. Gagniere, and J. Robert. Chem. Comm., 443 (1969).

40. G. Binsch. in Topics of Stereochemistry, Vol. 3. E.L. Eliel and N.L. Allinger (Editors). Interscience Pub., New York, 1968.

41. B.H. Barber. M.Sc. thesis, University of Manitoba, 1970.

42. M.A.H. Stewart. M.Sc. thesis, University of Manitoba, 1970.

43. B. Fuhr. M.Sc. thesis, University of Manitoba, 1969.

44. J. Sandstrom. Endeavour XXXIII, 111 (1974).

45. S. Glasstone, K.J. Laidler, and H. Eyring. Theory of Rate Processes. McGraw-Hill Book Co., New York, 1941.

46. NMR Quarterly 9 (1974), Perkin-Elmer.

47. R.R. Shoup, E.D. Becker, and M.L. McNeel. J. Phys. Chem. 76, 71 (1972).

48. B.G. Cox, F.G. Riddell, and D.A.R. Williams. J. Chem. Soc. (B), 859 (1970).

49. H.S. Gutowsky, J. Jonas, and T.H. Siddell, III. J. Am. Chem. Soc. 89, 4300 (1967).

50. R.C. Neumann, Jr., D.N. Roark, and V. Jonas. J. Am. Chem. Soc. 89, 3412 (1967).

51. R.C. Neumann, Jr. and V. Jonas. J. Am. Chem. Soc. 90, 1970 (1968).

52. K.J. Laidler. Chemical Kinetics. McGraw-Hill Book Co., Toronto, 1965, Chapter 3.

53. A. Steigel, J. Sauer, D.A. Klein, and G. Binsch. J. Am. Chem. Soc. 94, 2770 (1973).

54. L.L. Graham and R.E. Diehl. J. Phys. Chem. 73, 2696 (1969).

55. B. Nilsson, P. Martinson, K. Olsson, and R.E. Carter. J. Am. Chem. Soc. 96, 3190 (1974).

APPENDIX

Transformation of Spin Operators

Consider the spin angular momentum operators in the Cartesian coordinate system: I_x, I_y, I_z and I^2.

The commutation relationships show that only I^2 commutes with each of the other operators as well as with itself. Define an identity operator, ℓ, which also commutes with each of the above. We can write

$$\left[I^2,I_x\right] = \left[I^2,I_y\right] = \left[I^2,I_z\right] = \left[I^2,\ell\right] = 0$$

and

$$\left[I_x,I_y\right] = (I_xI_y - I_yI_x) = iI_z$$

$$\left[I_y,I_z\right] = iI_x$$

$$\left[I_z,I_x\right] = iI_y$$

Define a "raising" operator: $I_+ = I_x + iI_y$, and a "lowering" operator: $I_- = I_x - iI_y$ and determine their commutation relationships

e.g.
$$\left[I_z,I_+\right] = (I_zI_+ - I_+I_z) = I_z(I_x + iI_y) - (I_x + iI_y)I_z$$

$$= (I_zI_x + iI_zI_y - I_xI_z - iI_yI_z)$$

$$= (I_zI_x - I_xI_z) + i(I_zI_y - I_yI_z)$$

$$= \left[I_z,I_x\right] + i\left[I_z,I_y\right] = iI_y + i(-iI_x)$$

$$\left[I_z,I_+\right] = I_x + iI_y = I_+$$

i.e.
$$(I_zI_+ - I_+I_z) = I_+$$

$$I_zI_+ = I_+ + I_+I_z$$

Since $\ell x = x$ for all x, $I_+ = I_+\ell$

we can write $I_z I_+ = I_+ \ell + I_+ I_z = I_+(\ell + I_z)$

If more than one I_z value is possible, the value of a given s level is

$$I_z^s I_+ = I_+ \ell^s + I_+ I_z^s \qquad \text{(since } \ell^s = \ell \text{ for all s)}$$

or $$I_z^s I_+ = I_+(\ell + I_z)^s$$

Now multiply by the rotation factor for this single s value if the coordinates rotate with angular velocity, w. i.e. by $\frac{(-iwt)^s}{s!}$ (see note)

$$\frac{(-iwt)^s}{s!} I_z^s I_+ = I_+(\ell + I_z)^s \frac{(-iwt)^s}{s!}$$

To obtain the total effect, sum over all values from s = 0 to s = ∞

i.e. $$\sum_{s=0}^{\infty} \frac{(-iwtI_z)^s}{s!} I_+ = I_+ \sum_{s=0}^{\infty} \frac{\left[-iwt(\ell + I_z)\right]^s}{s!}$$

From Taylor's Theorem we have (Protter and Morray, p. 643)

$$e^x = e^a \sum_{s=0}^{\infty} \frac{(x - a)^s}{s!}$$

If a = 0 and x is the numerator in the above, one obtains

$$e^{-iwtI_z} I_+ = I_+ e^{-iwt(\ell + I_z)}$$

Since $e^{A + B} = e^A e^B$ if and only if $\left[A,B\right] = 0$ and since $\ell, I_z = 0$

one can write

$$e^{-iwtI_z} I_+ = I_+ e^{-iwt\ell} e^{-iwtI_z}$$

Multiplying from the right by e^{+iwtI_z}

$$e^{-iwtI_z} I_+ e^{+iwtI_z} = I_+ e^{-iwt\ell}$$

Recall $\ell x = x$ for all x, then e^{-iwt} is a scaler. Hence one obtains

$$e^{-iwtI_z} I_+ e^{+iwtI_z} = e^{-iwt} I_+$$

If we define $U = e^{-iwtI_z}$, then $U^{-1} = e^{+iwtI_z}$ to yield

$$U I_+ U^{-1} = e^{-iwt} I_+$$

Similarly $U I_- U^{-1} = e^{+iwt} I_-$

If the coordinate axes were to rotate in an opposite direction to the above, one would obtain

$$U^{-1} I_+ U = e^{+iwt} I_+$$

and $$U^{-1} I_- U = e^{-iwt} I_-$$

Note: w is in rad/sec.

t is in sec.

A similar transformation to rotating coordinates is given by N. M. Atherton in Electron Spin Resonance. John Wiley & Sons Toronto, 1973, pp. 273 ff.